



Jomo Kenyatta University of Agriculture and Technology
College of Engineering and Technology
School of Mechanical, Materials, and Manufacturing Engineering
Department of Mechatronic Engineering

Development of a cooling system for a liquid rocket engine

(FYP18-22)

FINAL PROJECT REPORT

Michael Kimani (ENM221-0066/2017)

Felix Wanyoike Gateru (ENM221-0056/2017)

Supervisors

Dr. Shohei Aoki

Dr. Bernard Owiti

Technologist

Mr. J Mbugua

December, 2022

Submitted in partial fulfillment of the requirements for the degree of Bachelor of Science in Mechatronic Engineering in Jomo Kenyatta University of Agriculture and Technology, 2022.

Declaration

We hereby declare that the work contained in this report is original; researched and documented by the undersigned students. It has not been used or presented elsewhere in any form for award of any academic qualification or otherwise. Any material obtained from other parties have been duly acknowledged. We have ensured that no violation of copyright or intellectual property rights have been committed.

1. Michael Kimani

Signature..... Date.....

2. Felix Wanyoike Gateru

Signature..... Date.....

Approved by supervisors:

1. Dr. Shohei Aoki

Signature..... Date.....

2. Dr. Bernard Owiti

Signature..... Date.....

Abstract

Operation of rocket engines involves combustion of propellants. The thermal energy produced during this combustion is integral to the rocket operation but can be detrimental to the structure of the rocket. There is therefore need to cool the rocket body and protect it from heat damage. A number of techniques have been developed for cooling the chamber and the nozzle. These techniques typically involve test firing of a liquid rocket to obtain results. The development of a cooling system is often done in parallel with the development of the thrust chamber which can lead to damage of the thrust chamber if the developed cooling system does not perform to the required level. This deters potential development of rocketry in the university and the country in general. The report highlights the development and fabrication of a closed loop control cooling system test rig to be used in testing the cooling system of a liquid rocket engine. The test rig eliminates the need for static firing to test the cooling of rocket engine thus promoting rapid prototyping. The test rig comprises of a liquid rocket engine that is mounted with a static cooling system. It comprises of sensors to measure the effectiveness of cooling as the cooling parameters are varied. Data was obtained from the system showing the possibility to achieve dynamic cooling of the liquid rocket engine. This was done by varying the flow rate of the coolant. The optimized cooling system will be used for the Nakuja project N4 rocket that aims to reach an altitude of 100km.

Contents

| | |
|---|------------|
| Declaration | I |
| Abstract | II |
| Table of contents | III |
| List of figures | VII |
| List of tables | IX |
| 1 Introduction | 1 |
| 1.1 Background | 1 |
| 1.2 Problem statement | 1 |
| 1.3 Objectives | 2 |
| 1.3.1 Main objective | 2 |
| 1.3.2 Specific objectives | 2 |
| 1.4 Justification of the study | 3 |
| 1.5 Scope | 3 |
| 1.6 Expected outcomes | 4 |
| 2 Literature review | 5 |
| 2.1 Liquid rocket engine operation | 5 |
| 2.2 Nozzle design and isentropic flow | 5 |
| 2.3 Rocket engine testing | 8 |
| 2.4 Need for cooling | 9 |
| 2.5 Types of cooling | 9 |
| 2.5.1 Film cooling | 10 |
| 2.5.2 Ablative cooling | 10 |
| 2.5.3 Radiation cooling | 11 |
| 2.5.4 Regenerative cooling | 11 |

| | | |
|----------|---|-----------|
| 2.6 | Heat transfer in the combustion chamber | 12 |
| 2.7 | Dynamic cooling | 17 |
| 2.8 | Design considerations for cooling | 18 |
| 2.8.1 | Propellant selection | 18 |
| 2.8.2 | Material selection | 18 |
| 2.8.3 | Selection of coolant | 19 |
| 2.8.4 | Selection of cooling passages geometry | 20 |
| 2.9 | Pressure drop in the cooling system | 22 |
| 2.10 | Water cooling on test stands | 23 |
| 2.11 | Previous work | 23 |
| 2.11.1 | New Mexico Institute of Mining and Technology Socorro, New Mexico [1] | 24 |
| 2.11.2 | Instituto Superior Técnico,Lisbon,Portugal [2] | 25 |
| 2.11.3 | Arizona State University [3] | 26 |
| 2.12 | Proof of concept | 28 |
| 3 | Methodology | 29 |
| 3.1 | Outline | 29 |
| 3.2 | Mechanical module | 29 |
| 3.2.1 | Introduction | 29 |
| 3.2.2 | Combustion chamber subsystem | 30 |
| 3.2.3 | Cooling assembly subsystem | 43 |
| 3.2.4 | Coolant plumbing subsystem | 52 |
| 3.3 | Electrical module | 59 |
| 3.3.1 | Design requirements | 60 |
| 3.3.2 | Pump selection | 60 |
| 3.3.3 | Conceptual design | 61 |
| 3.3.4 | Implementation of the design | 62 |
| 3.3.5 | Fabrication | 64 |

| | |
|--|-------------|
| 3.4 Control module | 65 |
| 4 Results and discussion | 66 |
| 4.1 Mechanical Module | 66 |
| 4.1.1 Engine assembly | 66 |
| 4.2 Electrical Module | 69 |
| 4.2.1 Printed Circuit Boards | 69 |
| 4.2.2 Casing and electronic assembly | 71 |
| 4.3 Control Module | 73 |
| 4.4 Cooling test results | 74 |
| 4.5 Design validation | 74 |
| 4.5.1 Fluid flow analysis | 74 |
| 4.5.2 Thermo-structural analysis | 77 |
| 4.6 Data analysis and Discussion | 78 |
| 4.7 Recommendations | 78 |
| 5 Conclusion | 80 |
| References | 81 |
| Appendices | i |
| A Part drawings | i |
| B Bugdet and timeplan | viii |
| B.1 Provisional budget | viii |
| B.2 Timeplan | viii |
| C Programming Code | ix |
| C.1 CEA output parser-Python code | ix |
| C.2 Nozzle sizing code-Matlab code | xii |
| C.3 Main control logic- C++ Code | xv |

| | |
|---|-------|
| D Design reference tables, charts | xxiii |
|---|-------|

List of Figures

| | | |
|-------------|--|----|
| Figure 2.1 | Liquid rocket engine test stand schematic | 8 |
| Figure 2.2 | Film cooling | 10 |
| Figure 2.3 | Regenerative cooling | 11 |
| Figure 2.4 | Temperature gradient of regeneratively cooled combustion chamber | 14 |
| Figure 2.5 | Regenerative cooling geometry | 21 |
| Figure 2.6 | Film cooling geometry | 22 |
| Figure 2.7 | Completed engine-Youngblood ,2005 | 24 |
| Figure 2.8 | Tecnico Lisboa completed engine design | 26 |
| Figure 2.9 | Chamber cross section- Arizona state University. | 27 |
| Figure 3.1 | Modular representation of entire cooling system | 29 |
| Figure 3.2 | Nasa CEA Software | 32 |
| Figure 3.3 | Graph of Temperature/Isp against O/F ratio | 33 |
| Figure 3.4 | Chamber and nozzle conceptual design | 33 |
| Figure 3.5 | Chamber geometry designed | 34 |
| Figure 3.6 | Chamber part drawing | 35 |
| Figure 3.7 | Nasa CEA Results | 36 |
| Figure 3.8 | Final Chamber geometry | 37 |
| Figure 3.9 | Final Chamber part drawing | 38 |
| Figure 3.10 | Chamber geometry final | 40 |
| Figure 3.11 | Fabricated aluminium engine | 42 |
| Figure 3.12 | Outer Wall- back | 45 |
| Figure 3.13 | Outer Wall- front | 46 |
| Figure 3.14 | Outer wall fabrication | 49 |
| Figure 3.15 | Fabricated Outer wall-back | 50 |
| Figure 3.16 | Fabricated outer wall- front | 51 |
| Figure 3.17 | 1/2 inch Nipple | 52 |
| Figure 3.18 | Piping system conceptual design | 53 |

| | |
|---|-----|
| Figure 3.19 Plumbing for cooling | 55 |
| Figure 3.20 Fittings | 56 |
| Figure 3.21 Tank fitting and ball valve | 57 |
| Figure 3.22 Pump image | 58 |
| Figure 3.23 Pump support design | 59 |
| Figure 3.24 Pump support fabricated | 59 |
| Figure 3.25 Power distribution | 63 |
| Figure 3.26 Pump circuitry | 64 |
| Figure 3.27 Heater circuit | 65 |
| Figure 4.1 3D Model of Liquid rocket engine | 66 |
| Figure 4.2 Fabricated liquid engine cooling system | 67 |
| Figure 4.3 Fabricated liquid engine cooling system front | 68 |
| Figure 4.4 Fabricated liquid engine cooling system back | 69 |
| Figure 4.5 Sensors PCB | 70 |
| Figure 4.6 Actuation PCB | 71 |
| Figure 4.7 Electronics assembly-top view | 72 |
| Figure 4.8 Electronics assembly-front view | 72 |
| Figure 4.9 Snippet of control algorithm | 73 |
| Figure 4.10 Data Visualization Dashboard | 73 |
| Figure 4.11 Pressure distribution | 75 |
| Figure 4.12 Velocity distribution | 76 |
| Figure 4.13 Thermo-structural analysis- Stress analysis | 77 |
| Figure 4.14 Thermo-structural analysis- Volumetric analysis | 78 |
| Figure A.1 Aluminium engine | ii |
| Figure A.2 Spacer | iii |
| Figure A.3 Outer Wall front | iv |
| Figure A.4 Outer Wall back | v |
| Figure A.5 Engine Support | vi |
| Figure A.6 Pump Support | vii |

List of Tables

| | | |
|-----------|--|------|
| Table 2.1 | Common propellant combinations | 18 |
| Table 2.2 | Properties of common rocket materials | 19 |
| Table 2.3 | Case study summary-Youngblood | 24 |
| Table 2.4 | Case study summary-Tecnico Lisboa | 25 |
| Table 2.5 | Case study summary- Arizona State University | 27 |
| Table 3.1 | Material selection consideration | 39 |
| Table 3.2 | Properties of Ethanol as a coolant | 47 |
| Table 3.3 | Properties of Ethanol as a coolant | 47 |
| Table 4.1 | Constant versus dynamic cooling results | 74 |
| Table 4.2 | Boundary conditions fluid flow analysis | 75 |
| Table 4.3 | Boundary conditions fluid flow analysis | 77 |
| Table B.1 | Budget | viii |
| Table B.2 | Time plan | ix |

1 Introduction

1.1 Background

A rocket is any type of jet propulsion vehicle that carries propellants required for combustion and subsequent development of thrust. The propellants are usually either in solid or liquid state. Combustion occurs in a part of the rocket referred to as the rocket engine.

The rocket engine generates thrust through this aforementioned combustion. Here a release of thermal energy is derived from the chemical reactions of the propellants. High temperature and high pressure gases result from the combustion of the propellants. These gases are then ejected at the rocket nozzle at high velocity [4].

Liquid rocket engines are fed with liquid propellants stored under pressure from tanks and into a thrust chamber. The type of propellant used is either a bipropellant or monopropellant. A bipropellant consists of a liquid oxidizer and a liquid fuel. A monopropellant contains both oxidizing and fuel species [5].

The combustion temperatures in a liquid rocket engine are very high and can be over 3000 °C. This is also accompanied by a high heat transfer rate from the gases to the chamber wall.

The high temperatures and high heat fluxes experienced are above those of engineering materials. Thus a cooling system is crucial for a rocket engine.

1.2 Problem statement

Iterative testing along with simulation is an important part of rocket development in order to find the optimal parameters for each rocket flight.

Testing of the cooling system of a liquid rocket engine and the different composition of the coolant to be used should not necessarily involve fabrication of a new thrust chamber.

Currently testing of the cooling system of a rocket engine requires performing of a static firing test. This leads to having a damaged thrust chamber should the cooling system not work according to the required specification on each test. Damaging a thrust chamber as a result of failure due to high temperatures leads to the need to fabricate a new thrust chamber which is resource consuming. As such there is need for a part of the test stand that is dedicated to cooling which would allow for dynamic changing of the cooling rate. To solve this a cooling system test rig with closed loop control was designed and fabricated to allow for testing without the need for static firing

1.3 Objectives

1.3.1 Main objective

To design and develop as part of a test rig, a closed loop control cooling system for a liquid rocket engine.

1.3.2 Specific objectives

1. To design and develop a mechanical structure for a thrust chamber with cooling facilities.
2. To design and develop an electrical system to power the sensors controller and actuator.
3. To develop and implement a control algorithm to achieve closed loop control of the cooling process.
4. To test the cooling system.

1.4 Justification of the study

Developing a closed loop control cooling system of a liquid rocket engine to be deployed on a test rig will eliminate the need to have static firing to test the efficiency of the onboard cooling system. This will reduce the strain on resources for iterative testing. The data points obtained from the testing will thereby be used to optimize the onboard cooling system.

1.5 Scope

This project will focus on developing a thrust chamber and a cooling system as part of a test rig specifically for the aforementioned thrust chamber.

1.6 Expected outcomes

The expected outcomes are:

1. Mechanical structure with consisting of a combustion chamber, nozzle and plumbing mechanism for cooling.
2. Electrical design to power the electrical system and transmit sensor values and control signals.
3. A control algorithm to stabilize performance of the cooling system.

2 Literature review

2.1 Liquid rocket engine operation

Rocket propulsion systems can be classified according to their energy source type that is: chemical, nuclear, solar. Chemical propulsion systems are the most prevalent and involve combustion to produce high energy exhaust gases. The exhaust gases are thermodynamically expanded to produce a high velocity exhaust whose reaction force is thrust. Chemical propulsion systems include solid propellant, liquid propellant and hybrid propellant systems. Liquid propellant systems offer the highest energy density. Liquid rocket engines are chemical propulsion systems where the propellants are either in liquid or gaseous form. The efficiency of a chemical propulsion system refers to its ability to convert the stored chemical energy of the propellants to kinetic energy of the exhaust gases.

2.2 Nozzle design and isentropic flow

A combustion chamber is designed to sustain combustion at the a specified pressure and propagate reacted gases towards the nozzle. The nozzle accelerates this flow to exhaust velocity and decreases the pressure of the flow to match the designed exit plane pressure. This operation is governed by the following assumptions [5]:

1. The working fluid is homogeneous in composition.
2. All the species of the working fluid are treated as gaseous. Any condensed phases (liquid or solid) add a negligible amount to the total mass.
3. The working fluid obeys the perfect gas law.
4. There is no heat transfer across any and all gas-enclosure walls; therefore, the flow is adiabatic.
5. There is no appreciable wall friction and all boundary layer effects may be neglected.

6. There are no shock waves or other discontinuities within the nozzle flow.

The above assumptions enable the use of isentropic flow relations in the nozzle. Stagnation conditions occur at the chamber where the pressure and the temperature are at maximum level and the flow velocity is assumed to be zero. As the flow expands isentropically the pressure and temperature drop while the velocity increases. In a typical de Laval nozzle (one with a converging and diverging section) the flow before the throat (the narrowest part of the nozzle) is subsonic while flow after the throat is supersonic. Thus the equation of rocket operation is given as shown in equation 2.1 [5].

$$F = \dot{m}v_e + (p_e - p_o)A_e \quad (2.1)$$

where

F = Thrust(N)

\dot{m} =mass flow rate(kg/s)

v_e = velocity of exhaust gases at exit(m/s)

p_e = pressure of the exhaust gases at exit(Pa)

p_o = ambient pressure(Pa)

A_e =area of the exit plane(m^2)

Assuming that the pressure at the exit plane is equal to the ambient pressure then:

$$F = \dot{m}v_e \quad (2.2)$$

Since the flow is isentropic equation 2.3 [5] may be shown to hold between any two nozzle sections x and y.

$$\frac{T_x}{T_y} = \left(\frac{p_x}{p_y} \right)^{\frac{k-1}{k}} = \left(\frac{v_y}{v_x} \right)^{k-1} \quad (2.3)$$

where

T = temperature(°C)

p = pressure(Pa)

v = velocity(m/s)

$k = \frac{C_p}{C_v}$ and as function of the combustion reaction

C_p = Specific heat at constant pressure(J/kg/K)

C_v = Specific heat at constant volume(J/kg/K)

The above equation demonstrates the relation between pressure and velocity at any point in the nozzle. As this flow is isentropic the pressure at any point x is a factor of the ratio Area of point x and the throat Area. The thrust and the area can be related via the equation 2.4 [5].

$$C_F = \frac{F}{p_1 A_t} \quad (2.4)$$

where

C_F = thrust co-efficient

F = thrust(N)

p_1 = chamber pressure(Pa)

A_t = throat area(m^2)

The thrust co-efficient is a factor of the propellants chosen and can be found using such software as Nasa CEA. With the throat area determined the geometry can be determined using isentropic flow equation 2.5 [5].

$$\frac{A}{A_t} = \left(\frac{k+1}{2} \right)^{-\frac{k+1}{2(k-1)}} \left[\frac{1 + (\frac{k-1}{2})M^2}{M} \right]^{\frac{k+1}{2(k-1)}} \quad (2.5)$$

where

M = local Mach number of the gases.

2.3 Rocket engine testing

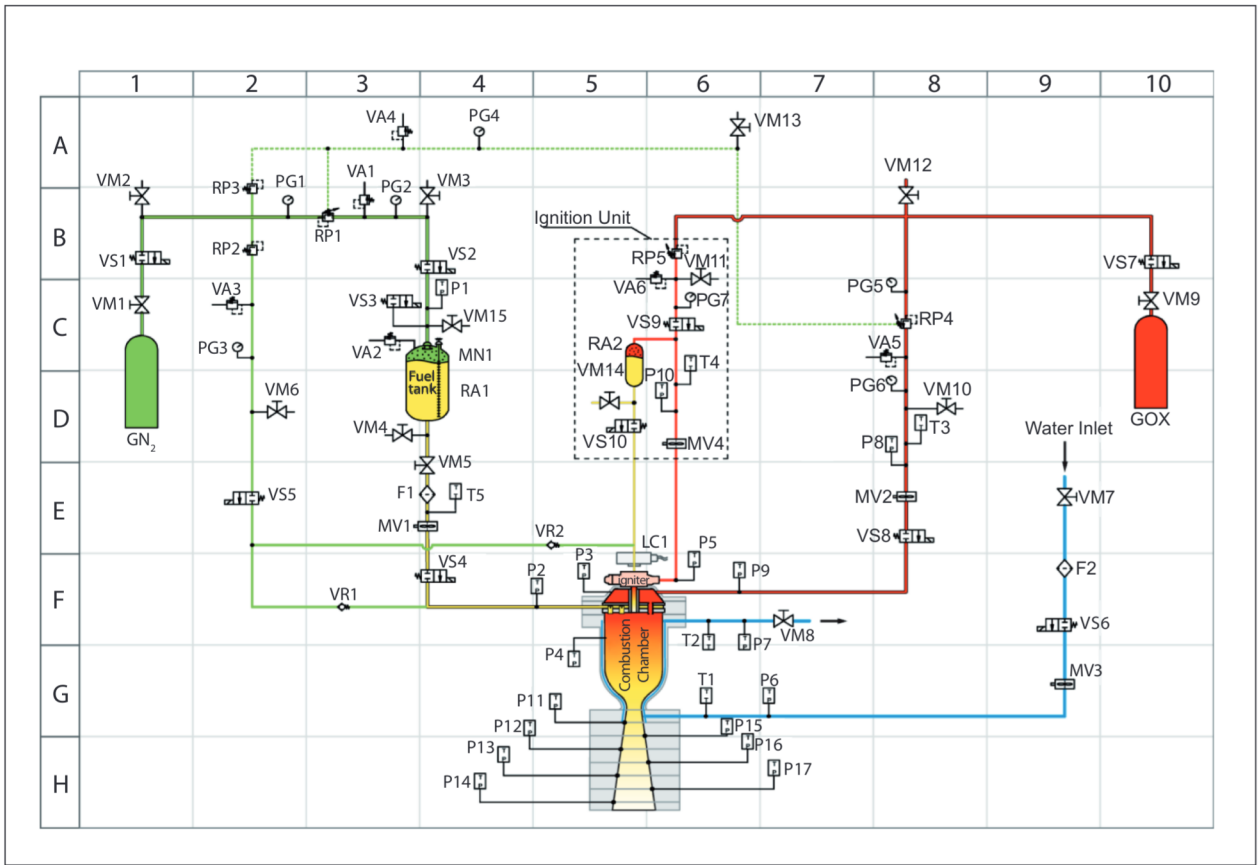


Figure 2.1: Liquid rocket engine test stand schematic[6]

To determine the rocket engine performance before the actual flight several tests are carried out on a test stand as represented in Figure 2.1 [7]. 2.1 demonstrates a bipropellant liquid rocket engine. Gaseous nitrogen in the green tank is used to pressurize the fuel towards the combustion chamber. The fuel used is ethanol (C_2H_5OH) which is stored in the fuel tank. Gaseous oxygen is the other propellant and is also used in the ignition unit. The ignition unit uses a small amount of the propellant mixture which is ignited when it reaches the igniter at the entrance of the combustion chamber. Water is pumped around the combustion chamber for cooling purposes. The entire schematic consists of manual, relief and solenoid valves that are used to control fluid flow. Flow meters are used to

measure the rate of fluid flow throughout the system [6]. The performance of the rocket engine is tested via a static test. The engine is clamped in place and ignited. The thrust produced is measured by force measuring devices such as load cells. The propellant feed system provides the propellant for the static firing [1].

2.4 Need for cooling

During rocket operation the propellants, oxidizer and the fuel, undergo combustion in the combustion chamber of the rocket. The reaction results in hot gases and is meant to liberate the chemical energy of the propellants, converting it into heat and pressure. If done stoichiometrically, combustion temperatures can range between 2500 to 3600 K for common propellants [5]. The combustion chamber and nozzle are designed to convert the heat and pressure generated into kinetic energy. The exhaust gases leave the nozzle at high velocity which generates a reaction force, thrust, which propels the rocket forward.

Not all the heat produced by the combustion is converted to kinetic energy. Some heat is absorbed by the combustion chamber and during nozzle operation a lot of the heat is dissipated to the nozzle. This is disadvantageous since most of the materials used to make rocket combustion chambers and nozzles lose strength as the temperature increases [3]. The chamber and nozzle also experience high pressure and if temperatures are allowed to rise this could lead to the material of the combustion chamber or nozzle failing or melting [8].

2.5 Types of cooling

Uncooled chamber walls can be used for a short duration up to a few seconds. For longer duration applications a cooling method has to be employed. Cooling methods can be characterized into two; steady state cooling methods and transient methods [5]. In steady state cooling methods heat transfer rates and chamber temperatures reach thermal

equilibrium. This include regenerative cooling and radiation cooling. In transient methods heat transfer rates and chamber temperatures do not reach thermal equilibrium, these methods include ablative cooling and film cooling [9].

2.5.1 Film cooling

Film cooling controls the chamber wall temperature by interposing a layer of coolant fluid between the surface to be protected and the hot gas stream from combustion as shown in Figure 2.2 [10]. This results in lower wall temperatures. It is used in high heat fluxes and in combination with steady state cooling methods such as regenerative cooling [11].

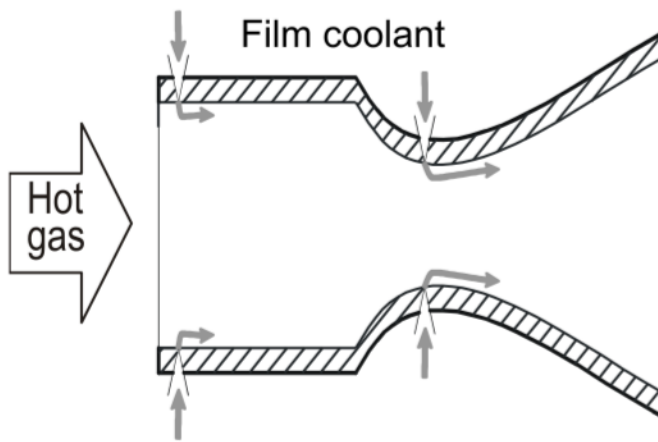


Figure 2.2: Film cooling [12]

2.5.2 Ablative cooling

Here select materials are used for sacrificial cooling by progressive endothermic disintegration of fiber-reinforced organic material and mass flow of pyrolysis gases away from the heated surface. This blocks heat transfer to the outer surface of the abrasive material [13]. This method suffers from two major challenges that is; the chamber is not reusable

as the wall material decomposes or disintegrates, the chamber geometry changes during operation thus optimum performance is not maintained.

2.5.3 Radiation cooling

The chamber is made of high temperature material. Heat is transferred away from the surface of the outer thrust chamber wall [4]. When it reaches thermal equilibrium, this wall may glow red or white as it radiates heat away to the surrounding medium or to empty space. This method is often used for small engines characterized by low pressure and low thermal fluxes [5].

2.5.4 Regenerative cooling

The fuel enters the cooling paths at the nozzle exit of the thrust chamber passes through the throat area and exits at the injector face as shown in Figure 2.3 [14]. This method is often used in applications with high chamber pressures and high heat transfer rates [15].

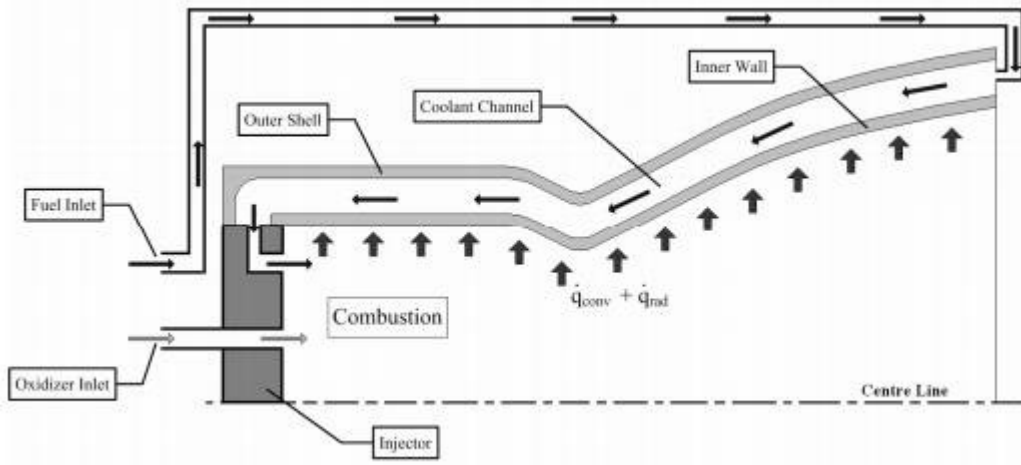


Figure 2.3: Regenerative cooling[16]

2.6 Heat transfer in the combustion chamber

Heat transfer analysis in the combustion chamber provide a useful guide in design, testing, and failure investigations [5]. Heat transfer analysis is different for steady state and transient cooling methods. Heat transfer analysis can be done by Finite Element Analysis (FEA) software. Heat transfer in the combustion chamber involves convection from the gases and propellants in the chamber, conduction by the chamber and nozzle and radiation from the surface of the nozzle and the chamber to the atmosphere. A majority of the heat transferred from the hot gases produced during combustion is transferred to the wall of the combustion chamber is done by convection. Conduction makes up a very small percentage with radiation accounting for between 5 - 35% [17] [18]. The basic relation of the heat transfer from the combustion gases to the wall of the combustion chamber can be expressed in equation 2.6 [17].

$$q = h_g(T_{aw} - T_{wg}) \quad (2.6)$$

where:

q = Heat flux; heat transferred across the stagnant gas film per unit surface per unit time.

h_g = Gas side heat transfer co-efficient.

T_{aw} = Adiabatic temperature of the gas.

T_{wg} = Hot-gas-side local chamber-wall temperature

The gas film co-effecient is given by equation 2.7 [17].

$$h_g = \left[\frac{0.026}{D_t^{0.2}} \left(\frac{\mu^{0.2} C_p}{Pr^{0.6}} \right)_{ns} \left(\frac{(P_c)_{ns} g}{c^*} \right) \left(\frac{D_t}{R} \right)^{0.1} \right] \times \left(\frac{A_t}{A} \right)^{0.9} \times \sigma \quad (2.7)$$

where

D_t = Diameter of nozzle throat

μ = Viscosity

C_p = Specific heat at constant pressure

Pr = Prandtl number

$(P_c)_{ns}$ = Stagnation pressure

c^* = characteristic velocity

R = Nozzle radius of curvature at throat

A = Area along chamber axis

σ = Correction factor for property variations across the boundary layer

A_t = Area of nozzle throat

The adiabatic temperature of the combustion gas at any given location in the thrust chamber can be obtained from equation 2.4.3 [17].

$$T_{aw} = (T_c)_{ns} \left[\frac{1 + r(\frac{\gamma-1}{2})M_x^2}{1 + (\frac{\gamma-1}{2})M_x^2} \right] \quad (2.8)$$

where:

$(T_c)_{ns}$ = Nozzle stagnation temperature

M_x = local Mach number

r = Local recovery factor

R = Effective recovery factor (from 0.90 to 0.98)

The local recovery factor represents the ratio of the frictional temperature increase to increase caused by adiabatic compression. This may be determined experimentally or estimated from equations 2.9 and 2.10[17].

$$r = 0.5Pr(\text{laminar flow}) \quad (2.9)$$

$$r = 0.33P_r(\text{Turbulent flow}) \quad (2.10)$$

Determination of gas side heat transfer co-efficient is a complex problem with data from analytical methods and experimental methods disagreeing [5] [18]. The disagreement is largely due to the initial assumptions of analytical methods than do not account for turbulent combustion pressure and the changing localised gas composition and temperature. The determination of heat flow is important in the analysis of the method of cooling to be chosen and the specific parameters.

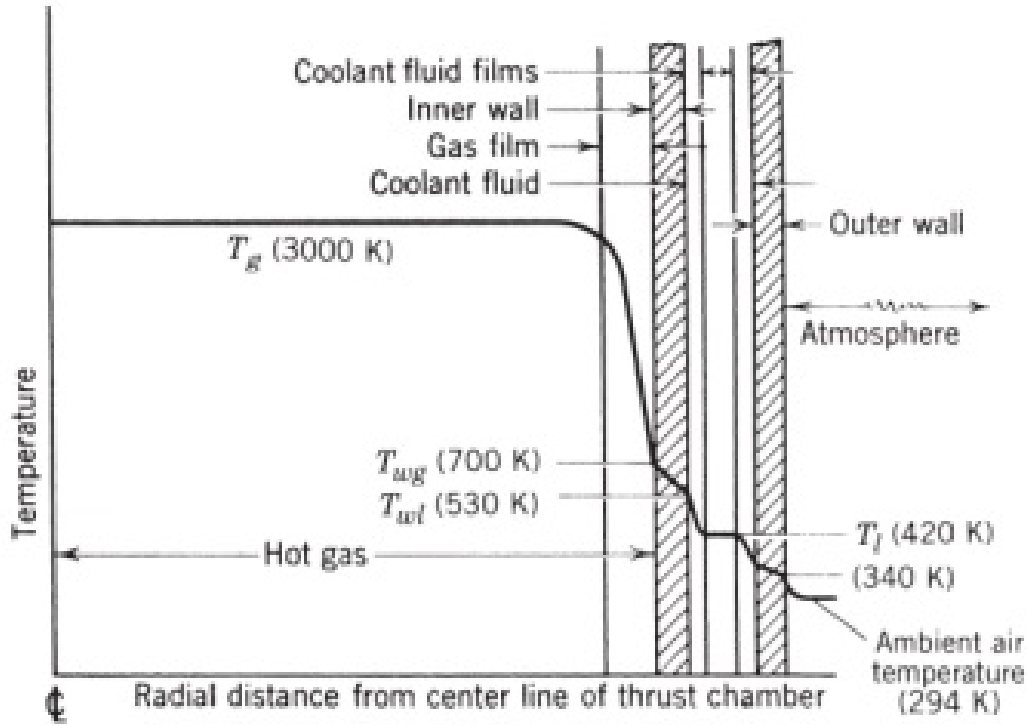


Figure 2.4: Temperature gradient of regeneratively cooled combustion chamber [5]

In the case of regenerative cooling as shown in Figure 2.4 the general heat transfer to the walls can be treated as a problem of steady state heat transfer in series. It is a combination

of convection at the boundaries of the flowing fluids and conduction through the chamber walls. The heat transfer involves convection through the gas film produced during combustion. The gas side heat co-efficient is found as detailed above [19]. This is followed by conduction through the wall of the chamber associated with the wall conduction co-efficient expressed by equation 2.11 [5].

$$\frac{Q}{A} = -k \frac{dT}{dL} = -k \frac{\Delta T}{t_w} \quad (2.11)$$

where:

Q = heat transferred to a surface area A

$\frac{dT}{dL}$ = temperature gradient

t_w = wall thickness and

k = thermal conductivity

The negative sign indicates that the temperature decreases as the thickness increases. This co-efficient is governed by the thickness of the wall and the thermal conductivity of the wall material. The third co-efficient in the series is the liquid film co-efficient of the coolant. Heat is transferred from the wall to the flowing coolant. The liquid film co-efficient denoted as h_l and is found as shown in equation 2.12 [17]:

$$h_l = \frac{kNu}{d} \quad (2.12)$$

where: Nu is Nusselt number and is given by equation 2.13 [17]:

$$Nu = C_1 Re^{0.8} Pr^{0.4} \left(\frac{\mu}{\mu_w} \right)^{0.14} \quad (2.13)$$

where:

C_1 = Constant (different values for various coolants)

Nu = Nusselt number

Re = Reynolds number = $\frac{\rho V_{co} d}{\mu}$

$$\text{Pr} = \text{Prandtl number} = \frac{\mu C_p}{k}$$

μ = Coolant viscosity at bulk temp.

μ_w = Coolant viscosity at coolant sidewall temperature.

d = Coolant passage hydraulic diameter.

k = Coolant thermal conductivity.

ρ = Coolant density.

V_{co} = Coolant velocity.

C_p = Coolant specific heat at constant pressure, These equation of convection heat transfer in turbulent flows are largely empirical, and can vary largely with actual experimental values. Th above equation is base on Bartz co relation which is semi-empirical. It offers a better estimation but actual values may vary. The general heat flux(q) can thus be calculated as in equation 2.14 and 2.15 [17]:

$$q = H(T_g - T_l) = \frac{Q}{A} \quad (2.14)$$

where:

q = heat transferred per unit area per unit time

T_l =the absolute coolant liquid temperature

and

$$H = \frac{1}{\frac{1}{h_g} + \frac{t}{k_w} + \frac{1}{h_l}} \quad (2.15)$$

where:

k_w = thermal conductivity of chamber wall

t = wall thickness

From the above equations it is possible to calculate the wall temperature. This relationship and the above bring a number of factors for cooling into the foreground[20]:

- The specific temperature of the coolant
- The specific heat capacity of the coolant
- The thickness of the chamber wall
- The nature of the propellants
- The nature of combustion including temperature and pressure
- The properties of the material used to make the chamber wall

2.7 Dynamic cooling

Cooling can be done at a constant or varying rate. Dynamic/variable cooling can be achieved by varying the mass flow rate of the coolant. This is highlighted by equation 2.12 where the liquid film co-efficient (h_l) depends on the Reynolds number which is affected by the mass flow rate of the coolant. An increase in the mass flow rate with a subsequent increase in velocity leads to an increase in the overall heat transfer coefficient [21].

2.8 Design considerations for cooling

2.8.1 Propellant selection

Table 2.1: Common propellant combinations [22]

| Oxidizer | Propellant | Isp(s) |
|---------------|----------------------|------------|
| Liquid oxygen | Kerosene | 250 to 270 |
| Liquid oxygen | Ethanol | 250 to 270 |
| Hydrazine | Chlorine trifluoride | 250 to 270 |
| Liquid oxygen | fluorine-JP-4 | 270 to 330 |
| Liquid oxygen | ozone-JP-4 | 270 to 330 |
| Liquid oxygen | Hydrazine | 270 to 330 |
| Liquid oxygen | fluorine-JP-4 | 270 to 330 |
| Fluorine | Hydrogen | 300 to 385 |
| Fluorine | Ammonia | 300 to 385 |
| Ozone | Hydrogen | 300 to 385 |
| Fluorine | Diborane | 300 to 385 |

A number of propellants are available for rocket propulsion which have been adequately studied and performance mapped as shown in Table 2.1. The main consideration for the selection of propellants was availability locally and relative safety in handling. Cryogenic propellants are not available locally hence the oxidizer chosen was gaseous oxygen instead of liquid oxygen.

2.8.2 Material selection

The material to be used to develop the combustion chamber and nozzle as well as the cooling jacket has a considerable effect on the cooling[3]. The material for design of the

combustion chamber should have the following characteristics:

- High thermal conductivity
- High melting point
- High specific thermal strength at high temperatures
- High wear resistance against erosion by exhaust gases
- Machinability

The properties of some common materials used in rocketry are as shown in 2.2 [23].

Table 2.2: Properties of common rocket materials [23]

| Metal | Density (g/cm^3) | Melting point | Cu 100 therm. conduc- tivity | chamber hard- ness | tensile strength at 1000 °C | nature of oxide at high temp |
|--------------------|-------------------------|------------------|---------------------------------------|--------------------------|--------------------------------------|---------------------------------------|
| Aluminium | 2.7 | 658 | 55 | 2.9 | liquid | refractory |
| Duralumin | 2.8 | 550 | 30 | 3.5 | liquid | refractory |
| Copper | 8.9 | 1083 | 100 | 3.5 | 10 MPa | powdery |
| Iron | 7.9 | 1538 | 30 | 4.5 | 18 MPa | powdery |
| Stainless steel | 7.8 | 1250 | 5 | 5.5 | 42 MPa | partial refrac- tory |

2.8.3 Selection of coolant

Depending on the type of cooling employed the type of coolant changes. For ablative cooling the material may be a solid ceramic. For film cooling the fuel is the coolant. For

transpiration cooling For regenerative cooling the coolant may be either the oxidizer or the fuel. Depending on the mass flow rate and the specific heat carrying capacity, one of the propellants is chosen. Despite the large temperature difference offered by liquid oxygen it offers compatibility issues [3].

2.8.4 Selection of cooling passages geometry

The geometry of the cooling passages has a large effect on the velocity of the coolant and the mass flow rate of the coolant. Thus the geometry of the cooling passages affect the heat transfer co-efficient to the coolant.

- **Regenerative cooling**

The cooling passages in regenerative cooling allow the flow of coolant through them during combustion. The coolant absorbs heat from the combustion chamber and this is used to preheat the propellant. The various types of cooling passages are as shown in Figure 2.5. Figure 2.5(a) shows circular tubes bounded by an outer shell. The circular tubes make up the combustion chamber and are reinforced by the outer shell. Figure 2.5(b) shows elongated tubes similar in operation to circular tubes with the only difference being the geometry of the passage. They are more effective than circular tubes due to the high aspect ratio. Figure 2.5(c) shows milled cooling channels as cooling passages. The assembly comprises of an inner combustion chamber than has milled channels on the outer side. The channels are covered by an outer shell which forms the closed geometry for cooling.

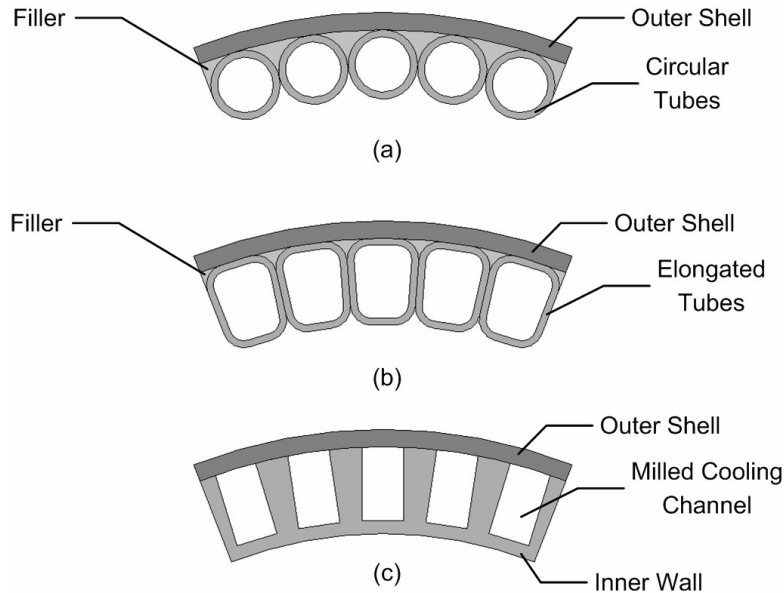


Figure 2.5: Regenerative cooling geometry[5]

The second technique involves the milling of rectangular cooling channels along the contour of a thick thrust chamber as shown in Figure 2.5.

- **Film cooling**

This type of cooling can be achieved using two techniques[24] The first involves the use of the injector. The injector configuration can be used to spray propellant onto the walls of the combustion chamber. The second method involve drilling holes or slots onto the wall of the combustion chamber to introduce the coolant. This is as shown in Figure 2.6.

- **Dump cooling**

Dump cooling involves the uses of cooling passages similar to those of regenerative cooling. The direction of coolant flow in dump cooling is opposite to that of regenerative cooling. The coolant is not used in combustion as in regenerative cooling.

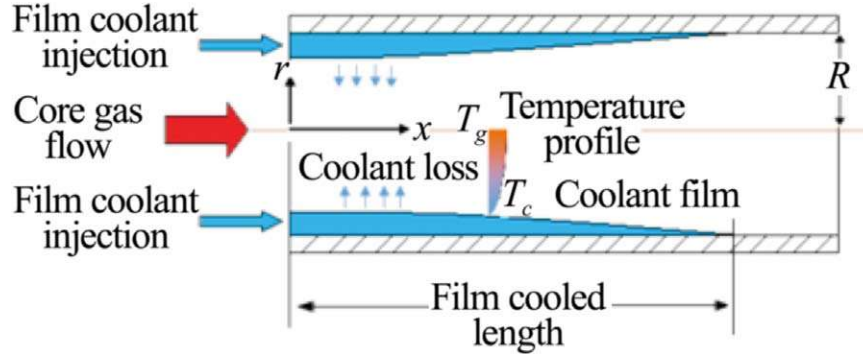


Figure 2.6: Film cooling geometry[24]

2.9 Pressure drop in the cooling system

The pressure drop in the cooling system is a major factor in design. It affects the choice of supporting machinery for the liquid engine such as turbo pumps. The pressure in the cooling channels also affects the rate of heat transfer in the cooling channels. The pressure drop in the cooling system can be calculated as shown in equation 2.16 [17].

$$\frac{\Delta p}{\rho} = \frac{1}{2} f v^2 \left(\frac{L}{D} \right) \quad (2.16)$$

where:

Δp = the friction pressure loss.

ρ = the coolant mass density.

L = the length of coolant passage.

D = the equivalent diameter.

v = the average velocity in the cooling passage.

f = a friction loss coefficient.

2.10 Water cooling on test stands

Here the temperature of the chamber wall is kept at a controlled temperature by running water at a constant rate through the cooling jacket. This is the same cooling jacket that would be used with a coolant during the flight of the rocket [6]. This process uses a constant mass flow rate which is determined using equation 2.17 [25].

$$m_w = \frac{1.1\pi q_{cw}(D_c + 2t_{cw})L_c}{c_w \Delta T_w} \quad (2.17)$$

where:

q_{cw} = Average heat transfer rate of chamber material.

D_c = Combustion chamber diameter.

t_{cw} = Thrust Chamber wall thickness.

L_c = Combustion chamber length.

c_w = Coolant water specific heat capacity.

ΔT_w = Desired water temperature value.

2.11 Previous work

The following section highlights previous work done relating to cooling systems for liquid rocket engines developed by other universities and institutions meeting the size requirements of the Nakuja project. The engine is to have a thrust of 2 kN.

2.11.1 New Mexico Institute of Mining and Technology Socorro, New Mexico [1]

The data from this case study can be summarized as follows:

Table 2.3: Case study summary-Youngblood

| Parameter | Value |
|------------------|--------------------|
| Fuel | Ammonia |
| Oxidizer | Nitrous Oxide |
| Thrust | 667N |
| Type of cooling | Radiation cooling |
| Chamber material | Oxygen Free Copper |

The completed rocket engine is as shown in Figure 2.7 [1]

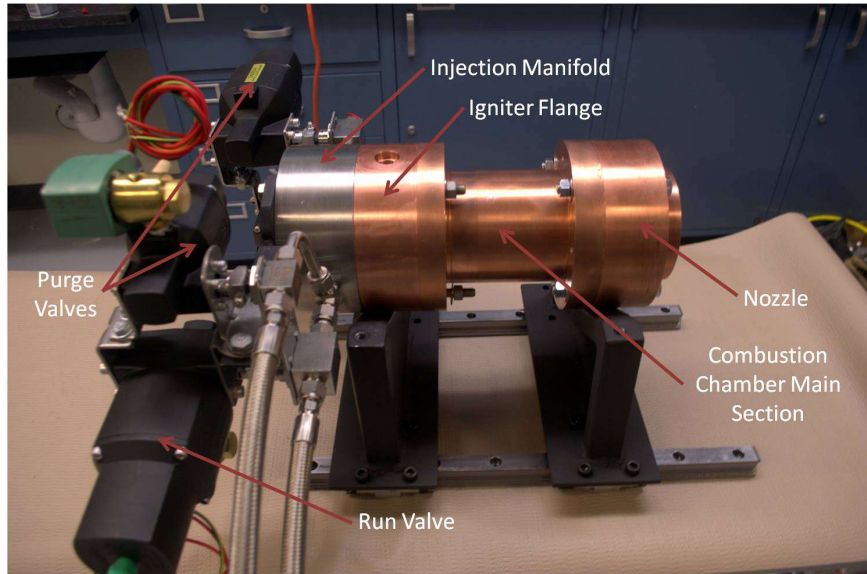


Figure 2.7: Completed engine-Youngblood ,2005

The major takeaways from this case study included:

- The design methodology used in the creation of the engine

- The type of data collection method employed during testing. The author insisted on using serial connections.
- The use of radiation cooling which was effective shows that it can also aid regenerative cooling.

2.11.2 Instituto Superior Técnico,Lisbon,Portugal [2]

The data from the case study can be summarized in table 2.4

[2]

Table 2.4: Case study summary-Tecnico Lisboa

| Parameter | Value |
|-------------------------------|---------------------------|
| Fuel | Ethanol |
| Oxidizer | Gas oxygen |
| Thrust | 25N |
| Type of cooling | Regenerative cooling |
| Regenerative cooling geometry | Coaxial shell |
| Chamber material | Stainless steel Grade 304 |

The completed engine is as shown in Figure 2.8:

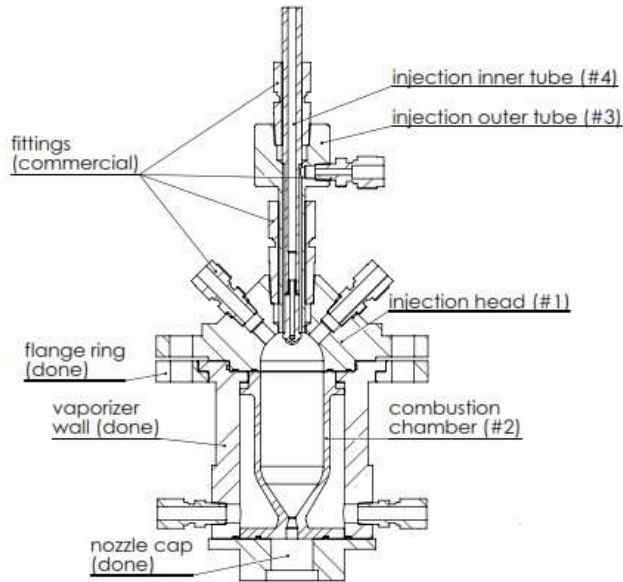


Figure 2.8: Tecnico Lisboa completed engine design

The major takeaways from this case study included:

- Ethanol was effectively used as a coolant with the temperature of the inner wall not exceeding the melting point of the chamber.
- The design involved the implementation of the coaxial shell regenerative cooling.

2.11.3 Arizona State University [3]

The data from the case study can be summarized as shown in table 2.5

[3]

Table 2.5: Case study summary- Arizona State University

| Parameter | Value |
|-------------------------------|----------------------|
| Fuel | Kerosene |
| Oxidizer | Liquid Oxygen |
| Thrust | 1.8 kN |
| Type of cooling | Regenerative cooling |
| Regenerative cooling geometry | Milled channels |
| Chamber material | Copper |
| Chamber pressure | 1.7 Mpa |

The completed engine is as shown in Figure 2.9

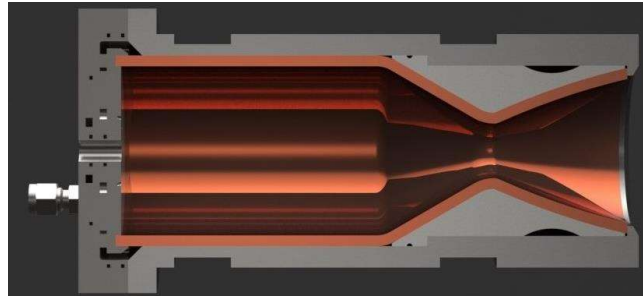


Figure 2.9: Chamber cross section- Arizona state University.

The takeaways from this study included:

- The report clearly highlighted the design procedure for a liquid rocket engine bringing into light concerns such as the convergence and divergence angles. The report also highlights a way to change the oxidizer to fuel ratio to achieve lower combustion temperatures
- The rocket was able to operate without failure with the exiting cooling

2.12 Proof of concept

The development of an appropriate cooling system for a liquid rocket engine is affected by a number of factors such as manufacturing constraints and engine specifications. For an efficient cooling system to be developed there is a necessity to test the developed cooling system. Existing systems require static tests. Static tests are resource intensive as they require firing the engine to test engine performance as well as cooling efficiency performance. Failure of the cooling system can be detrimental to the engine. There is need to develop a test rig that will be able to test cooling system performance without the need for static firing. This will present a cheap and efficient way of testing the cooling system.

3 Methodology

3.1 Outline

This section highlights design of the liquid rocket engine, the cooling system and the testing set up. It also highlights the mechanical, electrical and software design considerations and implementation. The system can be represented in modules as shown in Figure 3.1.

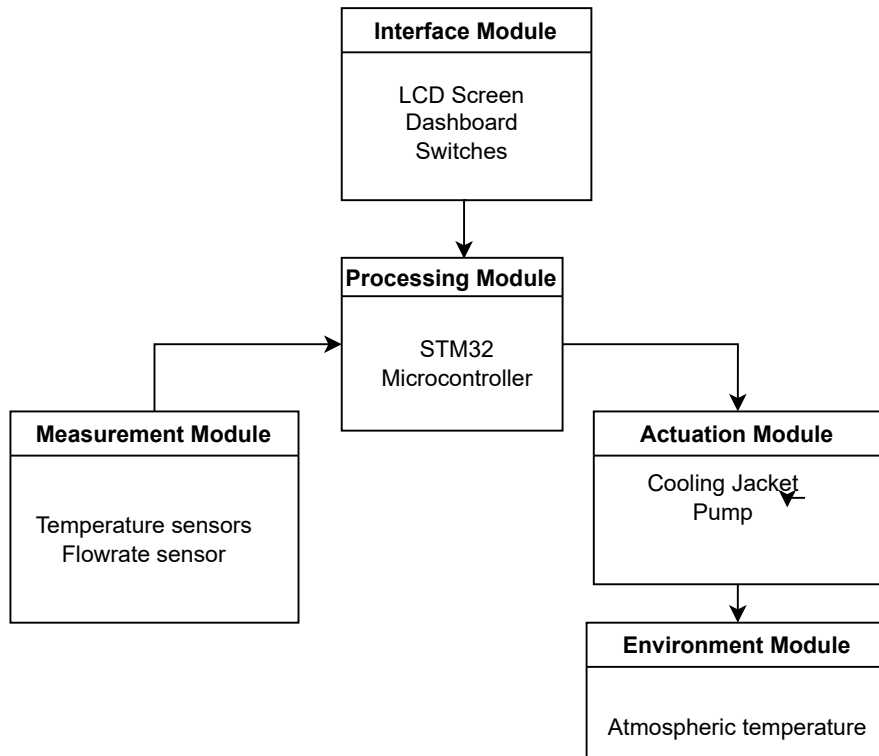


Figure 3.1: Modular representation of entire cooling system

3.2 Mechanical module

3.2.1 Introduction

The design fabrication of the mechanical module of the cooling system test rig is divided into the following subsections:

1. The combustion chamber subsystem
2. Cooling assembly subsystem
3. Fluid delivery subsystem

3.2.2 Combustion chamber subsystem

This subsystem is required to facilitate the combustion of the propellants(oxidizer and fuel). The products of the combustion are usually at high pressure and temperature and the combustion chamber subsystem is required to convert the high thermal energy and pressure into kinetic energy of the exhaust gases. This kinetic energy results into the thrust of the rocket. This subsystem comprises of the combustion chamber and the nozzle. The geometry of the combustion chamber and the nozzle have a great effect on the rocket performance and hence great care should be taken on the design. The design and fabrication followed the following steps:

1. Design requirements

The design requirements of the combustion chamber subsystem can be listed as:

- (a) Functional Requirements
 - i. The design should be able to handle the high temperatures of combustion which can be as high as 3300K [17] as well as high pressure of combustion.
 - ii. The design should offer high efficiency in the conversion of thermal energy and pressure into kinetic energy.
 - iii. The design should produce steady in-compressible flow without flow separation and supersonic flow at the exit.
- (b) Non-functional Requirements
 - i. The design should be able to be fabricated using locally available fabrication methods.

- ii. The design should be easily integrated into the injector and test stand design of the Nakuja project.

2. Design considerations

The following were design considerations for the design:

- Required thrust
- Combustion pressure
- Combustion temperature
- Propellants used
- Fabrication considerations

3. Conceptual design

The following steps were undertaken to generate a conceptual design:

- **Selection of propellants**

Cryogenic propellants are not available locally hence the oxidizer chosen was gaseous oxygen instead of liquid oxygen. Due to their availability and safety in handling, two fuels were considered, Kerosene and ethanol. Ethanol was chosen as it could be obtained with near 100% purity while the exact composition of Kerosene could not be determined.

- **Selection of specific Engine performance parameters**

As this project is part of the Nakuja project the following parameters were established as requirements.

- Chamber pressure = 2.0 Mpa
- Desired thrust = 2 kN

- **Selection of Oxidizer-Fuel ratio**

The oxidizer to fuel (O/F) ratio is an important parameter in the calculations to design the chamber geometry. The O/F ratio is also important in determining the mass flow rate of the propellants which also determines the cooling capability of the rocket. The determination of the O/F ratio requires determination of combustion parameters of the fuel and oxidizer. This was done using the NASA CEA software shown in Figure 3.2.

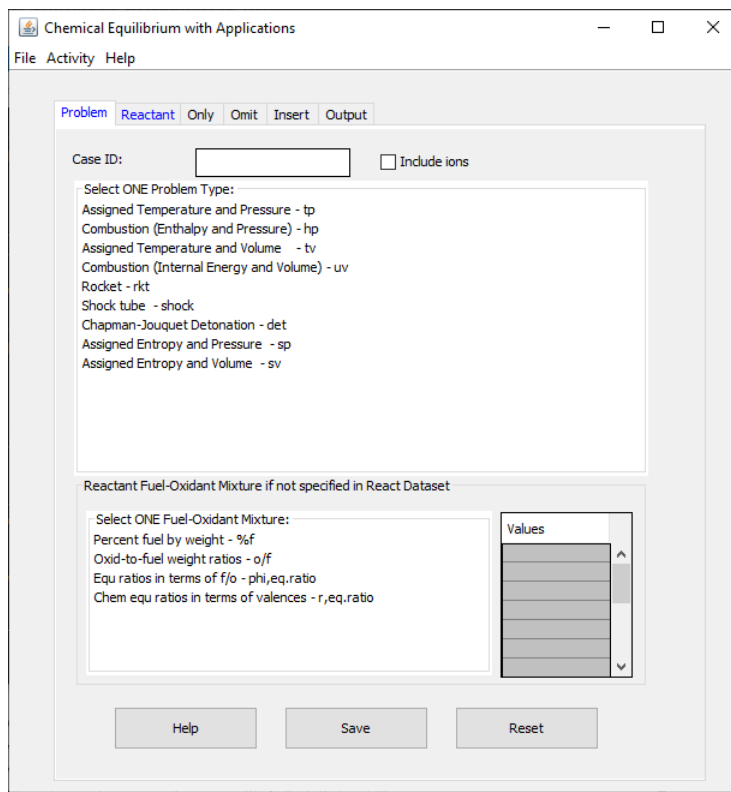


Figure 3.2: Nasa CEA Software

The software was able to generate data on various O/F ratios. A Python script was written to parse and data and generate graphs which would be used to pick the optimum O/F ratio. The main considerations for this selection were the specific Impulse (Isp) and the combustion temperature. The specific impulse is a measure of rocket performance and the higher the better. The combustion temperature was required to be kept at a minimum to limit material stresses.

The graphs generated are as shown in Figure 3.3.

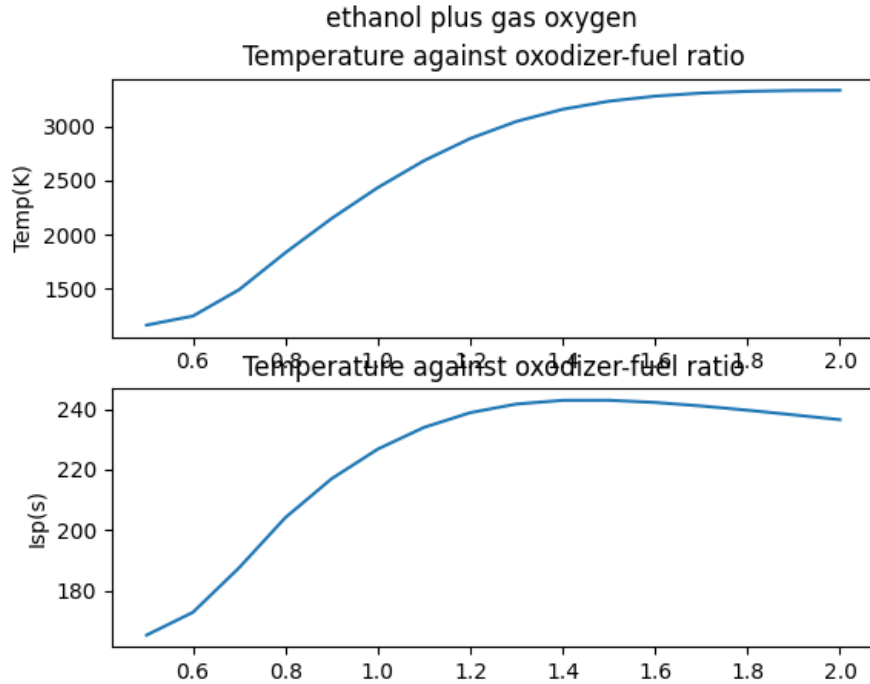


Figure 3.3: Graph of Temperature/Isp against O/F ratio

The optimum oxidizer to fuel ratio was chosen as 1.5. The conceptual design comprises a combustion chamber with a de Laval nozzle. This is as shown in Figure 3.4 which shows a simple converging, diverging section.

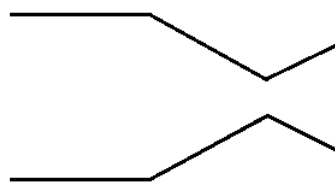


Figure 3.4: Chamber and nozzle conceptual design

4. Geometry design

The isentropic flow equations were used to determine the geometry. We generated a script to handle the calculations as shown in Appendix C. The calculations were confirmed using Rocket Propulsion Analysis (RPA) software which was also used to generate the parabolic approximation nozzle dimensions. The generated geometry is as shown in Figure 3.5.

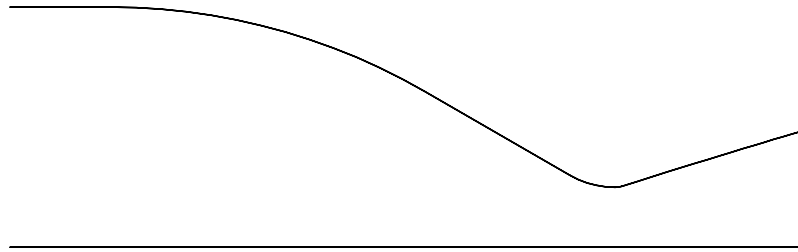


Figure 3.5: Chamber geometry designed

The geometry was produced in Autodesk Inventor and used to generate the combustion chamber. The generated drawing is as shown in Figure 3.6.

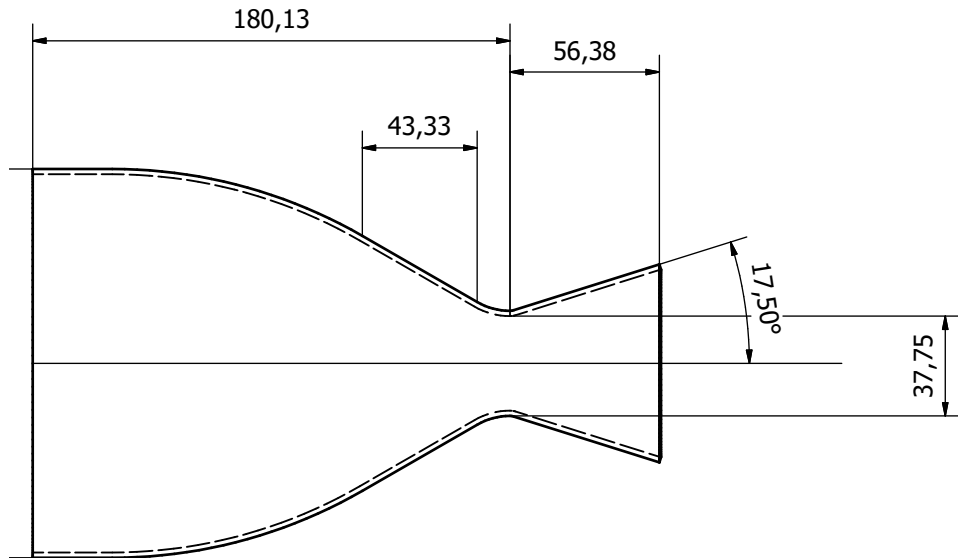


Figure 3.6: Chamber part drawing

Upon consultation and review of locally available fabrication methods it was determined that this geometry could not be achieved with existing production constraints. In order to maintain the integrity of the combustion chamber the piece had to be machined as one part. This greatly limited the fabrication options, requiring a 5 axis CNC machine which is not available. There was therefore the need for a redesign. The geometry was redesigned as follows:

Simulations of combustion conditions of ethanol and water were carried out using NASA CEA which generated values of Mach number as 22.036, Gamma as 1.133, characteristic velocity as 1738.5, as flow rate as 1.18703 as shown in Figure 3.7

| | CHAMBER | THROAT | EXIT |
|----------------------------|----------|----------|----------|
| Pinf/P | 1.0000 | 1.7312 | 22.222 |
| P, BAR | 20.000 | 11.552 | 0.90001 |
| T, K | 3232.25 | 3064.68 | 2256.37 |
| RHO, KG/CU M | 1.6399 0 | 1.0104 0 | 1.1023-1 |
| H, KJ/KG | -2410.66 | -3058.90 | -5556.22 |
| U, KJ/KG | -3630.26 | -4202.27 | -6372.68 |
| G, KJ/KG | -41747.5 | -40356.4 | -33016.4 |
| S, KJ / (KG) (K) | 12.1701 | 12.1701 | 12.1701 |
| M, (1/n) | 22.036 | 22.286 | 22.978 |
| (dLV/dLP)t | -1.02474 | -1.01881 | -1.00126 |
| (dLV/dLT)p | 1.4837 | 1.3885 | 1.0339 |
| Cp, KJ / (KG) (K) | 5.8444 | 5.2543 | 2.4928 |
| GAMMAS | 1.1330 | 1.1339 | 1.1819 |
| SON VEL, M/SEC | 1175.5 | 1138.6 | 982.3 |
| MACH NUMBER | 0.000 | 1.000 | 2.553 |
| PERFORMANCE PARAMETERS | | | |
| Ae/At | 1.0000 | 4.1609 | |
| CSTAR, M/SEC | 1738.5 | 1738.5 | |
| CF | 0.6550 | 1.4428 | |
| Ivac, M/SEC | 2142.8 | 2833.7 | |
| Isp, M/SEC | 1138.6 | 2508.2 | |

Figure 3.7: Nasa CEA Results

The diameter of the throat was obtained using the equation:

$$A_t = \frac{m}{P_s} \sqrt{\frac{T_o R}{\gamma}} \left(1 + \frac{\gamma - 1}{2}\right)^{\frac{\gamma+1}{2(\gamma-1)}} \quad (3.1)$$

where:

A_t = throat area(m^2)

m = mass flow rate(kg/s)

P_s = stagnation pressure(Pa)

R = universal gas constant

γ = combustion co-efficient.

Thus:

$$\begin{aligned} A_t &= \frac{1.18703}{2000000} \sqrt{\frac{3232.5 \times 377.305}{1.133} \left(1 + \frac{1.133 - 1}{2}\right)^{\frac{1.133+1}{2(1.133-1)}}} \\ &= 1031.916959 mm^2 \end{aligned} \quad (3.2)$$

The throat diameter was determined as 36.25. A characteristic chamber length of 2 was chosen thus making the volume of the chamber $2063.833918mm^2$. The chamber diameter was then determined to be thrice the nozzle diameter to keep the chamber diameter manageable. The chamber diameter was then obtained as 108.75 mm. The chamber geometry was further defined by:

$$\begin{aligned} A_e &= 4.168(\text{Obtained from Nasa CEA}) \times 1031.916959 \\ &= 4301.029885mm^2 \\ D_e &= 73.94mm \end{aligned} \quad (3.3)$$

The length of the chamber was calculated via geometry to yield 191 mm. The convergence and divergence angles were chosen as 30° and 15° respectively. These parameters generated the geometry shown in Figure 3.8

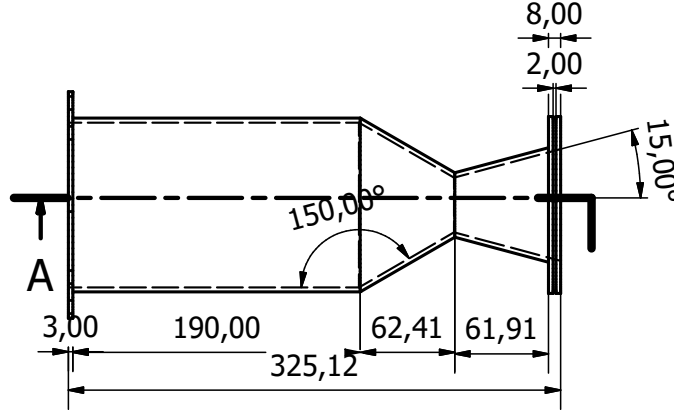


Figure 3.8: Final Chamber geometry

The complete part drawing is shown in Figure 3.9

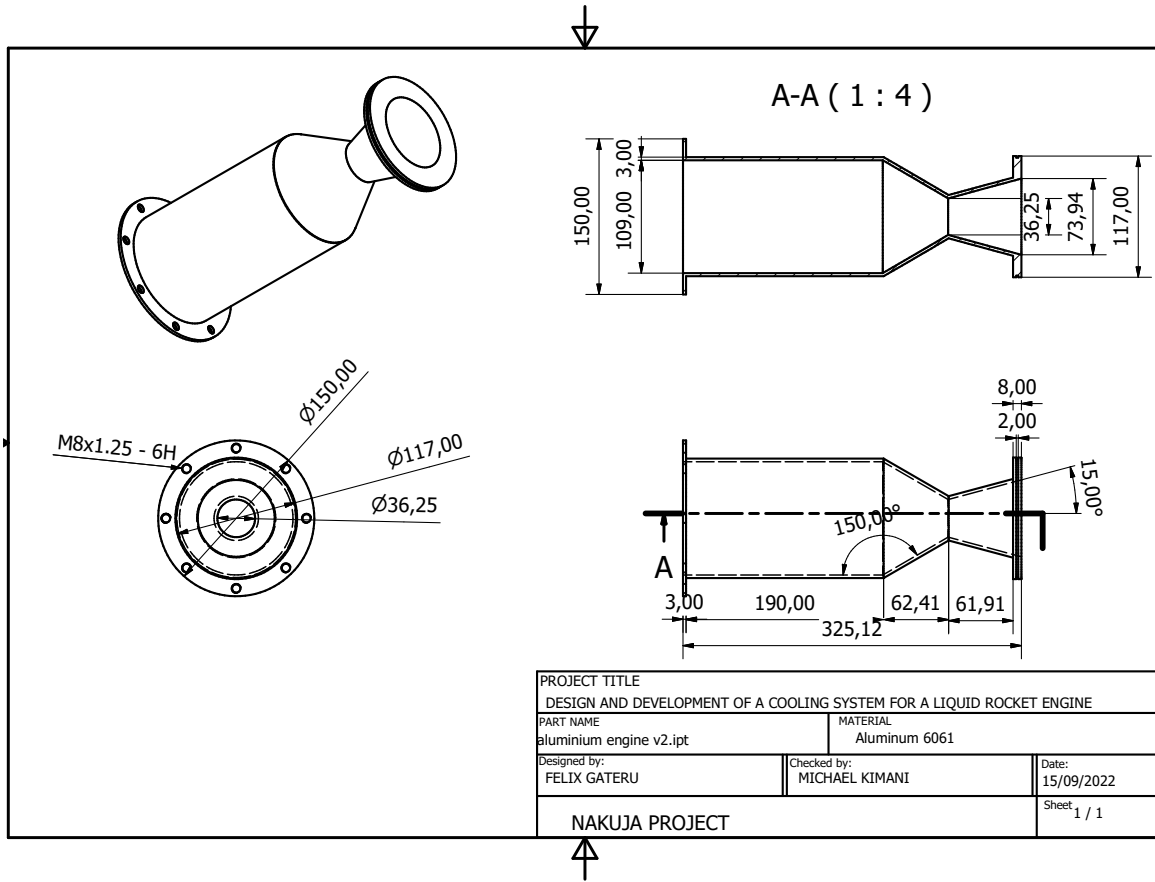


Figure 3.9: Final Chamber part drawing

5. Material selection

The following were requirements for the material to be selected for the chamber and nozzle:

- (a) High strength
- (b) High thermal conductivity
- (c) Machinability

The materials considered are as shown in Table 3.2.2:

Table 3.1: Material selection consideration

| Material | Tensile strength(MPa) | Melting point(°C) | Thermal Conductivity |
|---------------------------|-----------------------|-------------------|----------------------|
| Copper | 221 | 1083 | 391 W/m-K |
| Aluminium 7075 | 510 | 457 | 130 W/m-K |
| Aluminium 6061 | 600 | 276 | 167 W/m-K |
| Stainless steel Grade 304 | 540 | 1400 | 16.2W/m-K |

Aluminium 6061 was chosen because of its high thermal conductivity which offers a high rate of heat transfer. Copper was not chosen because of price and local availability constraints. The material chosen influenced the chamber geometry by determining the thickness of the chamber wall. The chamber wall is required to be thin to allow for effective heat transfer but still be strong enough to withstand the high combustion pressure. The design should also take into account the effect of elevated heat on the material. The chamber thickness was calculated as follows:

$$P_D = \frac{2 \times t \times fty \times 1000}{d \times s} \quad (3.4)$$

where:

t = thickness

fty = yield strength

d = chamber diameter

s = design safety factor

$$2000 = \frac{2 \times t \times 138 \times 1000}{109 \times 2}$$

$$t = \frac{2000}{1503.39} \quad (3.5)$$

$$t = 1.5 \times 2$$

$$t = 3mm$$

The chamber thickness in order to withstand at least 2MPa of pressure should be at least 3 mm shown in equation 3.5

The final design of the chamber is as shown in Figure 3.2.6.

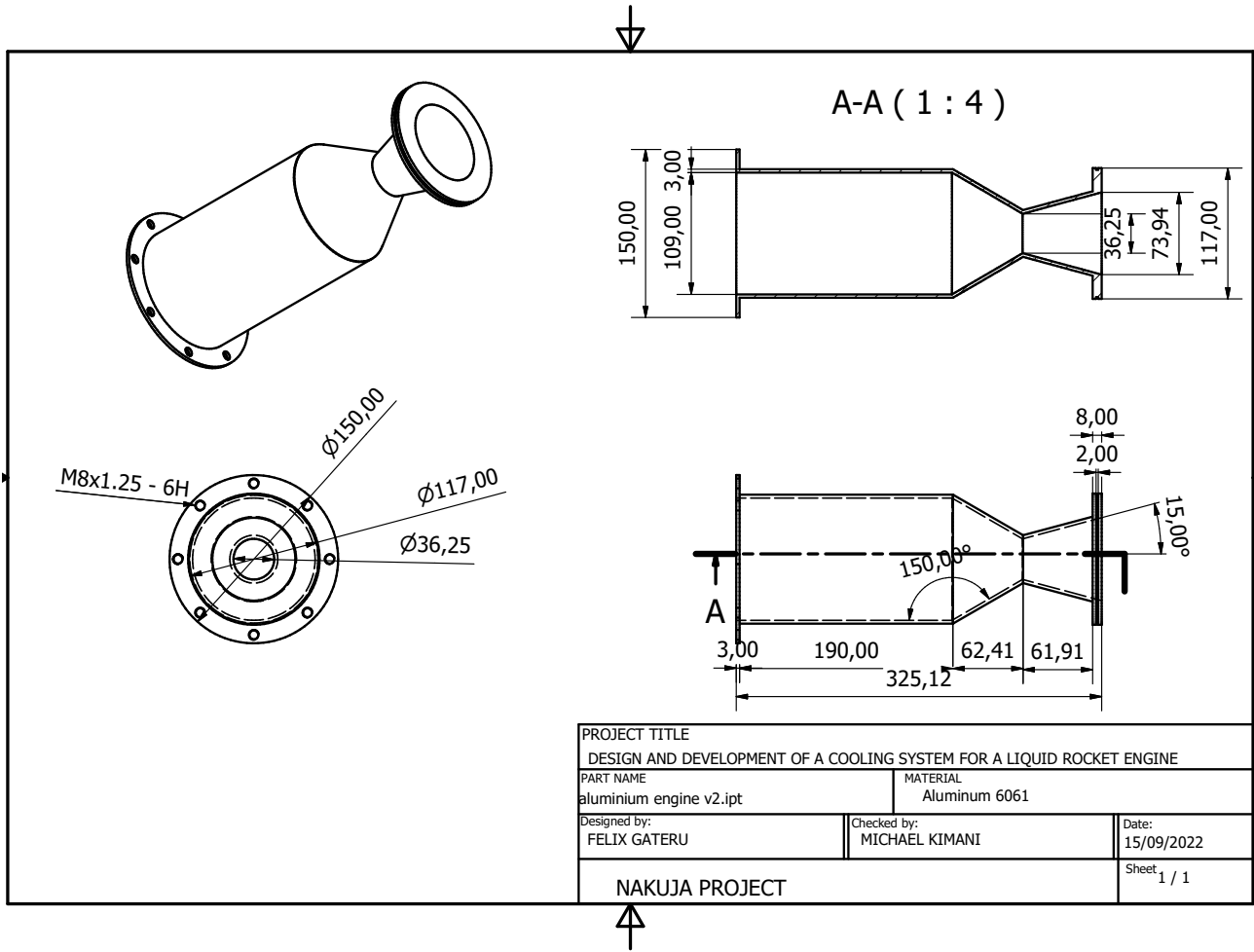


Figure 3.10: Chamber geometry final

6. Design validation

Validation of chamber design was done to ensure that the design met the technical requirements and that it was safe. The following validation procedures were conducted on the design:

- Fluid flow analysis Flow through a rocket engine nozzle is considered isentropic that is; it is adiabatic and reversible. Isentropic flow calculations can be conducted to determine the pressure and velocity of exhaust gases at any point

along the chamber geometry. These calculations are enhanced using CFD software such as ANSYS. The developed geometry was analyzed to determine exit pressure and the presence of shock waves and flow separation. The procedure was as follows:

- (a) A 2D axis symmetrical model of the chamber wall was imported into ANSYS.
- (b) The geometry was subjected to meshing.
- (c) Boundary conditions were applied
- (d) The simulation was run with 4500 iterations

The results are presented in chapter 4.

- Thermo-structural analysis The inner wall of the rocket engine will be subjected to both high temperature and pressure. Thermo-structural analysis is a combination of thermal analysis as well as static structural analysis. This is used to determine stresses under both pressure and thermal loading. The procedure was as follows:

- (a) A 3D model of the inner wall was imported into ANSYS.
- (b) The material was set for model and meshing was conducted.
- (c) Data from fluid flow analysis was imported to apply pressure and thermal loading.
- (d) The simulation was run with 6000 iterations

The results are as presented in chapter 4.

7. Design implementation

The internal taper on the engine geometry presented a fabrication issue with the current school facilities thus the fabrication of this part was outsourced to NMC. The final part is as shown in Figure



Figure 3.11: Fabricated aluminium engine

3.2.3 Cooling assembly subsystem

The cooling assembly subsystem is required to take away heat from the engine during operation to prevent failure of the chamber wall. From the literature review, regenerative cooling was chosen for the engine. It presents the following advantages:

- It is a relatively efficient method of cooling.
- It enables a method of dynamic control thus can be optimized for flight.
- The fuel used is preheated thus increasing the energy of combustion.
- It is relatively easy to implement.

The cooling assembly subsystem comprises of the inlet manifold, the outlet manifold and the outer wall. The following describes the steps for designing the regenerative cooling assembly:

1. Design requirements

The following were identified as design requirements for the cooling assembly subsystem:

- Functional requirements
 - (a) The system should be able to provide adequate cooling to the engine to prevent failure.
 - (b) The system should be able to vary the rate of cooling to optimise fluid flow
 - (c) The system should limit the pressure drop across the cooling channels.
- Non-functional requirements
 - (a) The system should be easy to implement.
 - (b) The system should not be bulky.

2. Design considerations

The following were design considerations for the cooling assembly subsystem:

- The combustion temperature of the propellants
- The enthalpy of the propellants
- The thermal conductivity, melting point and material of the combustion chamber,
- The pressure drop across the cooling channel.
- The type of regenerative cooling method implemented.
- The coolant and its properties.

3. Conceptual design

Following the requirements and design considerations of the subsystem, a regenerative cooling system using cooling tubes was proposed. Regenerative cooling was chosen due to its high efficiency. Cooling tubes were chosen because of fabrication constraints. The cooling tubes can be fabricated with the currently available resources.

4. Final design

The final design of the cooling subsystem was as shown below. It comprises of the front and back outer chamber with holes to accomodate for half inch pipe fittings. The parts are as shown in Figures 3.12 and 3.13.

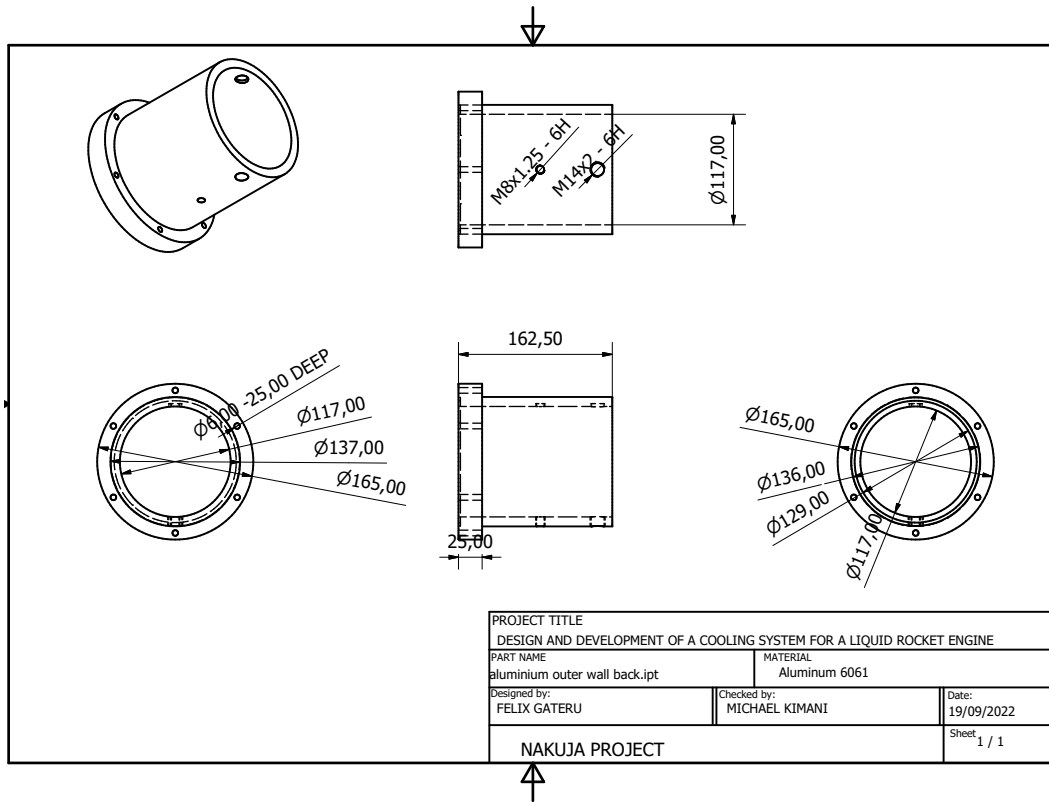


Figure 3.12: Outer Wall- back

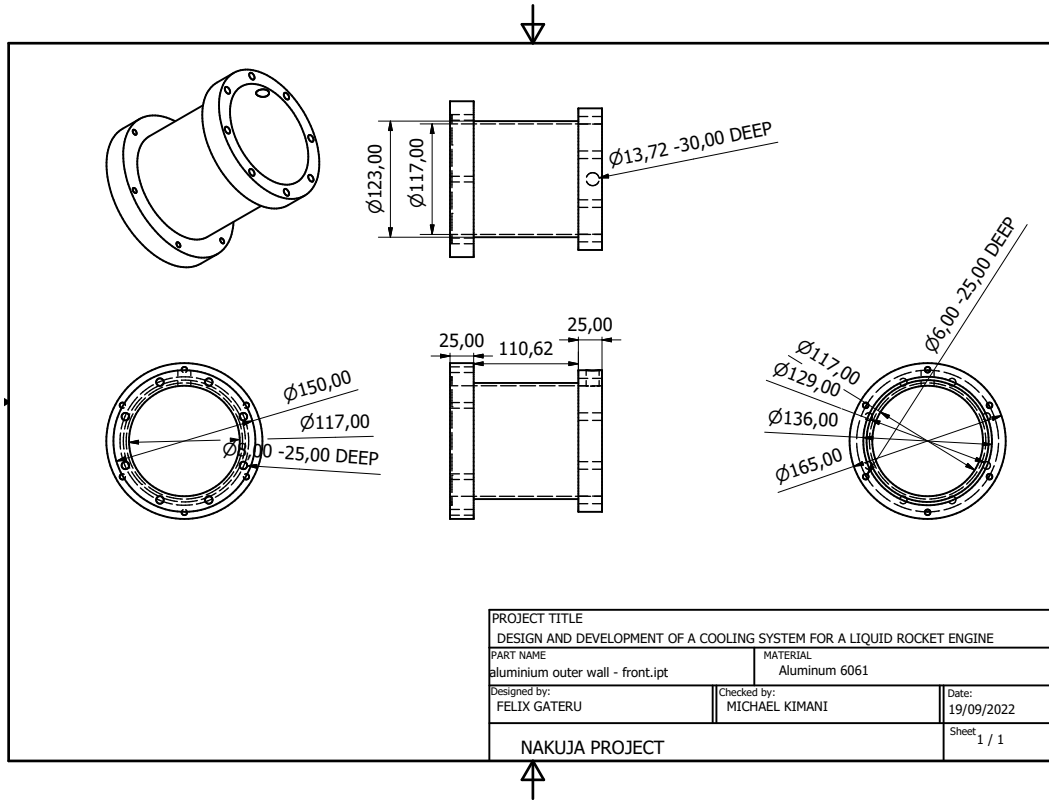


Figure 3.13: Outer Wall- front

5. Design implementation

- **Selection of coolant**

From the decision to use Gaseous Oxygen(GOX) and ethanol as the propellants, ethanol was chosen as the propellant to be used for regenerative cooling. Ethanol was used as it has a higher specific heat capacity than GOX. The pressure loss associated with GOX are much higher than that of ethanol. Some of the properties of ethanol are as listed in Table 5

Table 3.2: Properties of Ethanol as a coolant [26]

| Property | Value |
|------------------------|------------|
| Boiling point | 78.37 °C |
| Melting point | -114.1 °C |
| Specific heat capacity | 2.46 J/g°C |
| Thermal conductivity | 0.17 W/m-K |

To verify design and for preliminary testing, water was to be used instead of ethanol as it is non-flammable, easier to obtain than ethanol and cheaper.

Table 3.3: Properties of Ethanol as a coolant [26]

| Property | Value |
|------------------------|-------------|
| Boiling point | 100.00 °C |
| Melting point | 0.0 °C |
| Specific heat capacity | 4.184 J/g°C |
| Thermal conductivity | 0.598 W/m-K |

- **Cooling jacket**

The use of aluminium as the chamber wall material necessitates the use of a robust form of regenerative cooling to take away the heat. This due to the fact that aluminium has a relatively high conductivity and has a relatively low melting point. As a result a coaxial shell cooling geometry was selected. From the geometry design we obtained an outer wall of diameter 115 mm. The cooling jacket is required to facilitate passing of coolant over the surface of the combustion chamber to take away the heat.

- **Material selection**

Aluminium 7075 was chosen as the material for the cooling jacket as it is corrosion resistant to both ethanol and water. Aluminium is also

lightweight and has good machinability offering the ability to make complex geometries relatively easily.

– **Geometry design**

Cooling jacket inner diameter should be equal to the outer diameter of the combustion chamber plus the height of the cooling film. The coolant film was designed to have a height of 1mm. This presented the highest cooling efficiency as shown by the graph below(insert cooling) The design of the cooling jacket is as illustrated below. The cooling jacket is to be made into two parts as it is too long to machine as one piece with existing fabrication constraints..(Insert the design of the cooling jacket) The outer chamber also comprises of fittings to allow for fluid to enter into the cooling cavity from the fluid delivery system.

– **Design implementation**

The two parts of the cooling jacket were fabricated as follows demonstrated by Figure 3.14:



Figure 3.14: Outer wall fabrication

- (a) Aluminium 7075 of diameter 175 mm was cut to a length of 200mm.
- (b) The piece was machined on the lathe in the order of facing to obtain datum, facing to the required dimension, drilling and then boring to final internal dimensions. Finishing operations on the lathe included the use of a file and sand paper to obtain a good surface finish.
- (c) Drilling of holes for the bolts was then done. The final process involved drilling and tapping of holes on the circumference.

The final part is as shown in the Figures 3.15 and 3.16



Figure 3.15: Fabricated Outer wall-back



Figure 3.16: Fabricated outer wall- front

A 1/2 inch nipple is used to connect the cooling sub assembly to the fluid delivery system. This is as shown in figure 3.17.



Figure 3.17: 1/2 inch Nipple

3.2.4 Coolant plumbing subsystem

The main aim of the coolant delivery subsystem is to deliver the coolant at high pressures and allow distribution into the cooling tubes. The subsystem is also responsible for collecting the spent coolant in the case of the test stand. The design of this subsystem was as follows:

1. Design requirements

The design requirements of the coolant plumbing subsystem can be described as

- Functional requirements
 - (a) The pump should be able to deliver the coolant to the channels at the required flow rate
 - (b) The subsystem should offer a way to integrate sensors for parameter measurement,

- (c) The subsystem should be able to achieve dynamic cooling by varying the flow rate of the pump.
- Non-functional requirements
 - (a) The subsystem should be easy to assemble.
 - (b) The subsystem should offer a fail safe mechanism.

2. Design considerations

The following were design considerations for the coolant plumbing subsystem:

- The mass flow rate of the coolant through the system.
- The sensors to be used to measure coolant properties.
- The size of the tubing used to deliver the coolant.
- The size of the pump in the system

3. Conceptual design

The design requirements and considerations led to development of one conceptual design. The conceptual design comprises of two reservoirs, a pump and the connecting tubes to and from the engine. The design is as shown below:

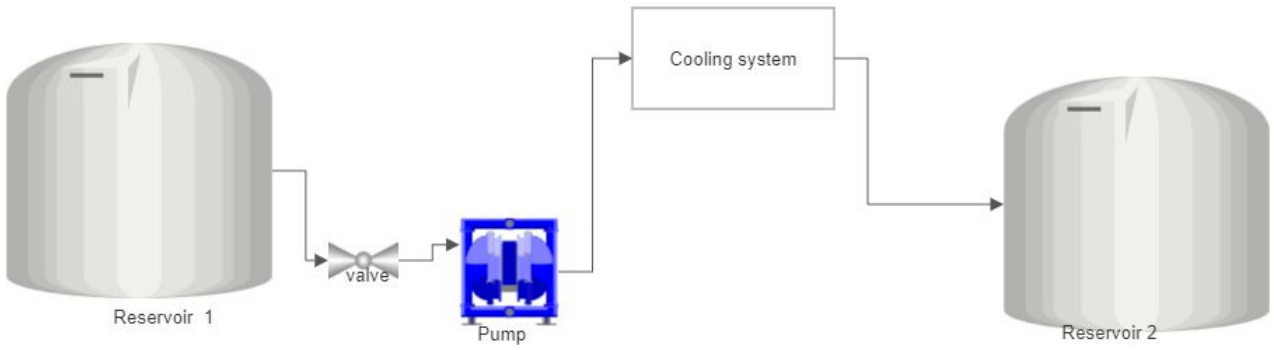


Figure 3.18: Piping system conceptual design

4. Final design

- **Tank selection**

The main considerations for the selection of the tank were the running time of the system and the need to incorporate sensors. The tank geometry was chosen to utilize readily available tanks. The calculations for tank geometry were as follows:

$$\text{Mass flow rate of coolant} = 0.5 \text{ kg/s}$$

$$\text{Proposed running time} = 5 \text{ minutes}$$

$$\begin{aligned} \text{Mass} &= 0.5 \text{ kg/s} \times 60 \times 3 \\ &= 90 \text{ kg} \end{aligned} \tag{3.6}$$

$$\text{Density of ethanol} = 789 \text{ kg/m}^3$$

$$\begin{aligned} \text{volume} &= \frac{\text{mass}}{\text{density}} \\ &= \frac{90 \text{ kg}}{789 \text{ kg/m}^3} \\ &= 0.114 \text{ m}^3 \\ &\approx 0.12 \text{ m}^3 \end{aligned} \tag{3.7}$$

Two metal drums of capacity 200l were selected as they met the requisite capacity. A metal drum was preferred as ethanol is a highly volatile liquid hence a metallic drum would be easier to cool than one made from plastic.

- **Plumbing design**

The plumbing for cooling purposes was done as shown in figure 3.19

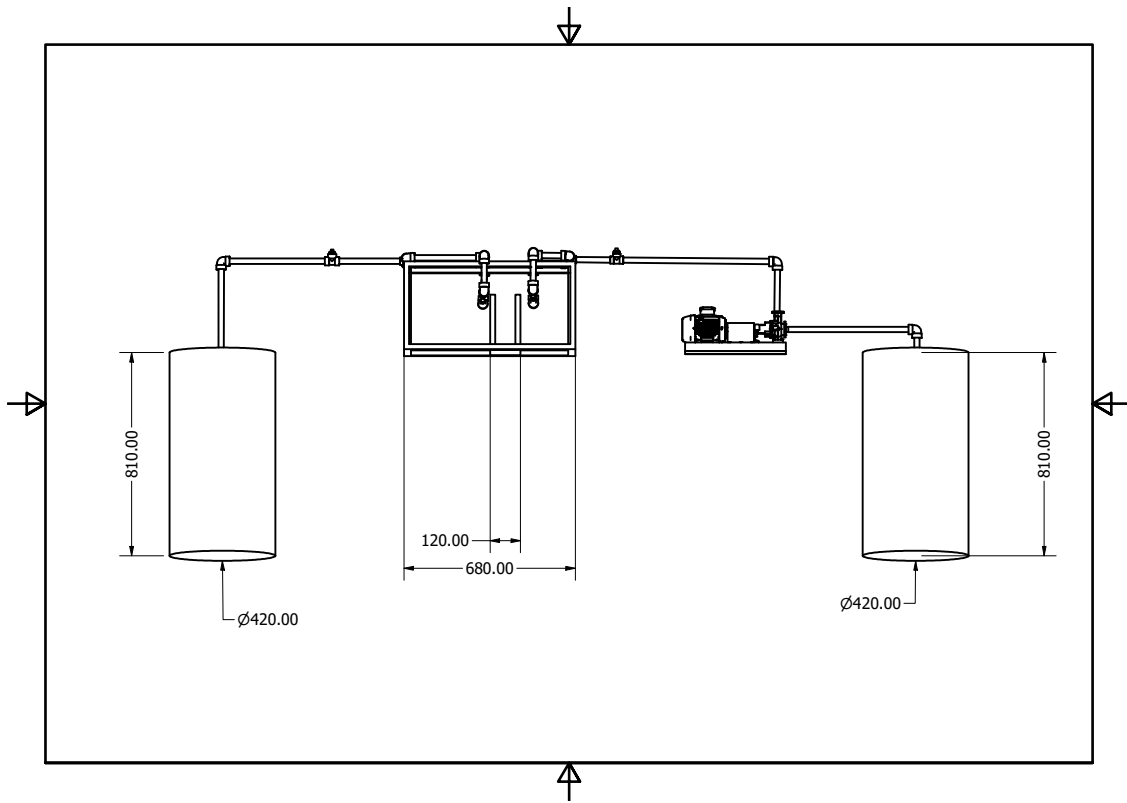


Figure 3.19: Plumbing for cooling

5. Design implementation

The plumbing system was fabricated as follows:

- (a) Holes were drilled at the bottom of one of the tanks and a 1 inch tank fitting used.
- (b) One inch PVC pipes were used to connect the tank fitting to the pump.



Figure 3.20: Fittings

- (c) From the outlet of the pump one inch PVC was joined to a reducer and a 1/2 inch nipple connected to allow the fitting of a 1/2 inch pipe to the cooling assembly. As shown in figure 3.21



Figure 3.21: Tank fitting and ball valve

- (d) A 1/2 inch pipe with a 1/2 inch nipple was used as the outlet from the cooling subsystem to the tank. An image of the pump is as shown in Figure

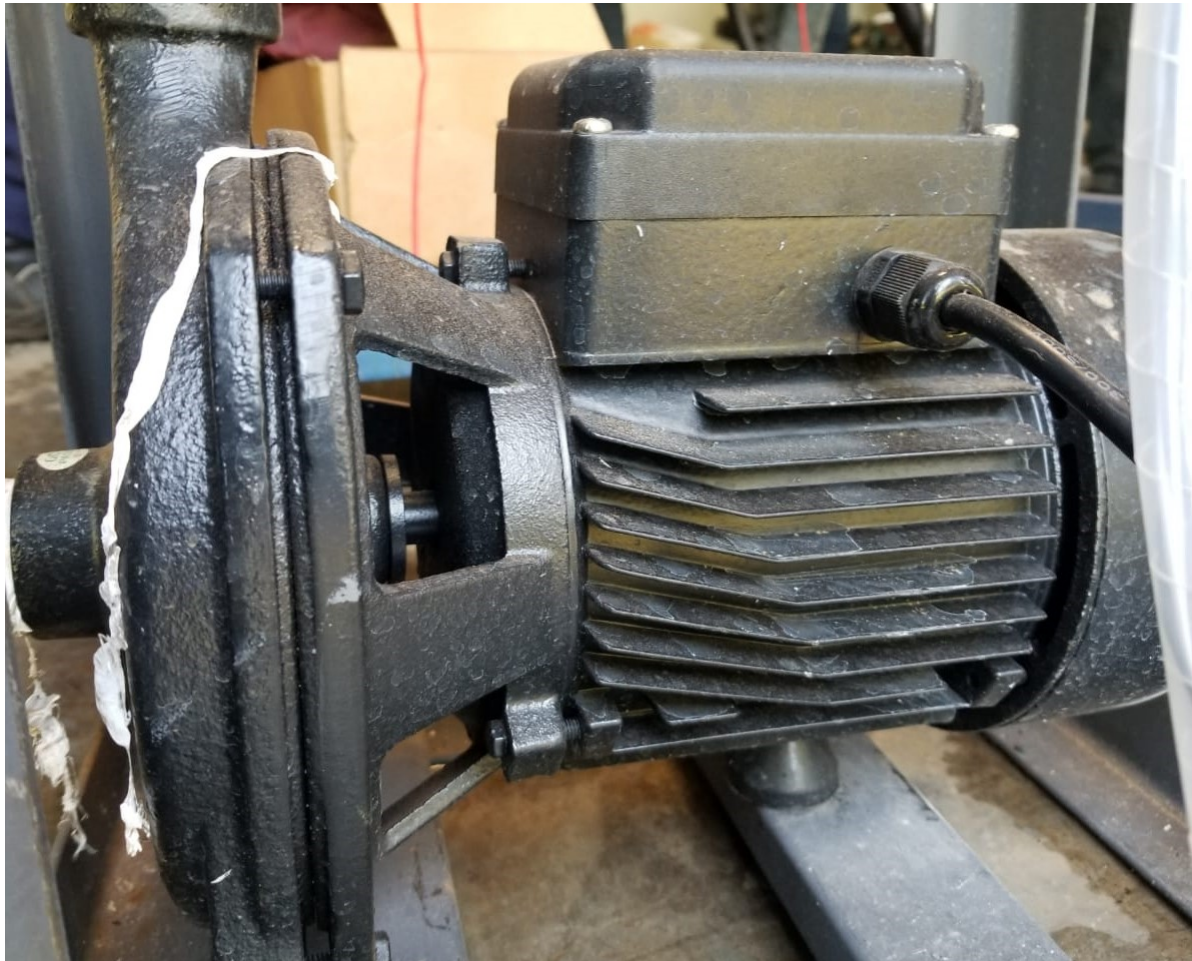


Figure 3.22: Pump image

- (e) The use of the pump necessitated the design of a pump housing to support the pump. The deign and implementation are as shown in Figure 3.23 and 3.24

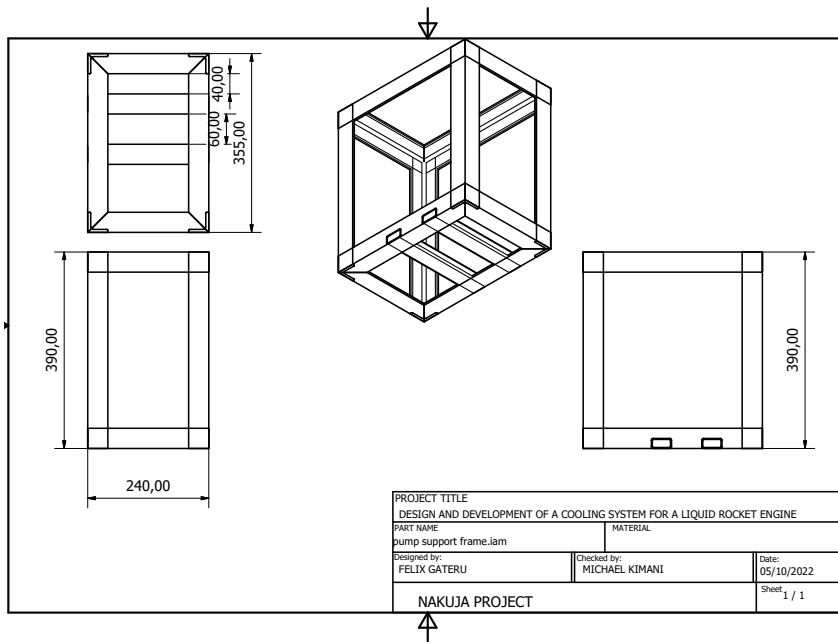


Figure 3.23: Pump support design



Figure 3.24: Pump support fabricated

3.3 Electrical module

The electrical module is designed to enable varying of the flow rate of the coolant via the pump in order to achieve dynamic cooling. The electrical module aims to achieve

delivery of power to the various electrical components and transmit electrical signals from the sensors to the controller and actuation signals from the controller to the actuator in form of the pump and heater.

3.3.1 Design requirements

1. Functional requirements
 - (a) The electrical module should facilitate for delivery of appropriate power and allow for variation of power delivered to the pump for flow rate control.
 - (b) The electrical module should allow for an interface to receive user inputs and display outputs to the user.
 - (c) The electrical module should allow for delivering of appropriate power to the microcontroller and sensor suite.
 - (d) The electrical module should allow for powering and control of a heater in order to facilitate for testing of the cooling system.
2. Non-functional requirements
 - (a) Power efficiency
 - (b) Safety
 - (c) Minimum heat dissipated
 - (d) Indicator lights
 - (e) Aesthetically pleasing connections

3.3.2 Pump selection

The considerations were:

1. Flow rate

The fuel mass flow rate as a design point is 0.5161kg/s. The choosing of this value is beyond the scope of this project. This in cubic metres per hour is shown in equation 3.8 below.

$$\begin{aligned}
 volume &= \frac{massflowrate}{density} \\
 &= \frac{0.47481\text{kg/s}}{789\text{kg/m}^3} \\
 &= 6.0179 * 10^{-4}\text{m}^3/\text{s} \\
 &= 2.166\text{m}^3/\text{hr}
 \end{aligned} \tag{3.8}$$

2. Viscosity of the fluid

Highly viscous fluids are more suited to positive displacement pumps while fluids with low viscosity like fresh water are more suited to centrifugal pumps.

A centrifugal pump with a maximum flow rate value of $7\text{m}^3/\text{hr}$ was chosen. This allows for more than thrice the base flow rate allowing for testing of the cooling over a wide range of flow rates.

3.3.3 Conceptual design

The conceptual design comprises of:

1. Power distribution circuit

The design considerations include:

- (a) Should avail appropriate power in terms of voltage and current to each of the components from the main power supply.
- (b) Incorporate safety features to prevent damage to the components.
- (c) Design should protect from electrical noise to ensure the signal integrity is maintained throughout the circuit.

- (d) Allow for manual overrides to the system in the event of a power emergency

2. Pump circuitry

The design requirements include:

- (a) Should provide 1248W maximum power to pump the cooling fluid at the desired variable rates from $2.166m^3/hr$, the fuel base flow rate to $7m^3/hr$ which is the maximum flow rate achievable by the pump.
- (b) Should fit well into the mechanical structure.

3. Sensors

These sensors are as follows:

- (a) Temperature sensors
- (b) Pressure sensors

The design considerations will be:

- (a) The sensors should provide accurate and consistent data.
- (b) The sensors should be compatible with the chosen microcontroller.
- (c) Temperature sensors should achieve the required range from 24 °C to 700 °C.

4. User interface.

The user interface should appropriately and promptly relay communication from the system to the user and allow for inputs from the user into the system.

3.3.4 Implementation of the design

1. Power distribution

The power distribution schematic is shown in Figure 3.25 below. Appropriate power is delivered to the microcontroller, sensors, LCD interface and to the pump. AC

power through the mains is rectified to DC power to power the microcontroller and the sensors.

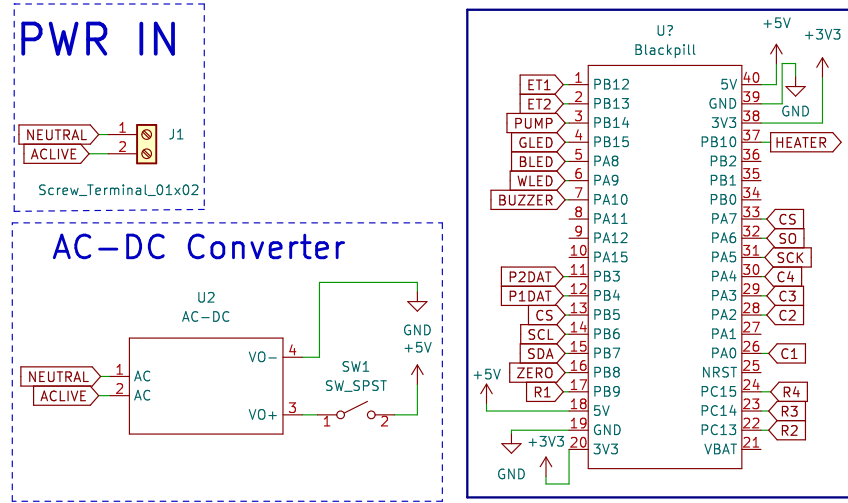


Figure 3.25: Power distribution

2. Pump circuitry

The pump circuit schematic is as shown in Figure 3.26. The pump circuitry allows for provision of power at variable rates to the pump. A Triac is used for switching purposes. The voltage is varied by varying the firing angle of each cycle of the supply alternating current current. This is done after detecting the zero crossing point detection of each alternating current cycle.

3. Heater circuit

The heater circuit allows for turning on and off of the heater using commands from the microcontroller. As the heater is used for testing purposes, the above is a safety measure in the event of an anomaly in the sensor data. The heater circuit comprises of an optocoupler for switching as shown in Figure 3.27 for electrical isolation purposes.

4. Printed Circuit Boards

To achieve the above functionalities the above circuits were all implemented in two circuit boards. One circuit board included the sensor con-

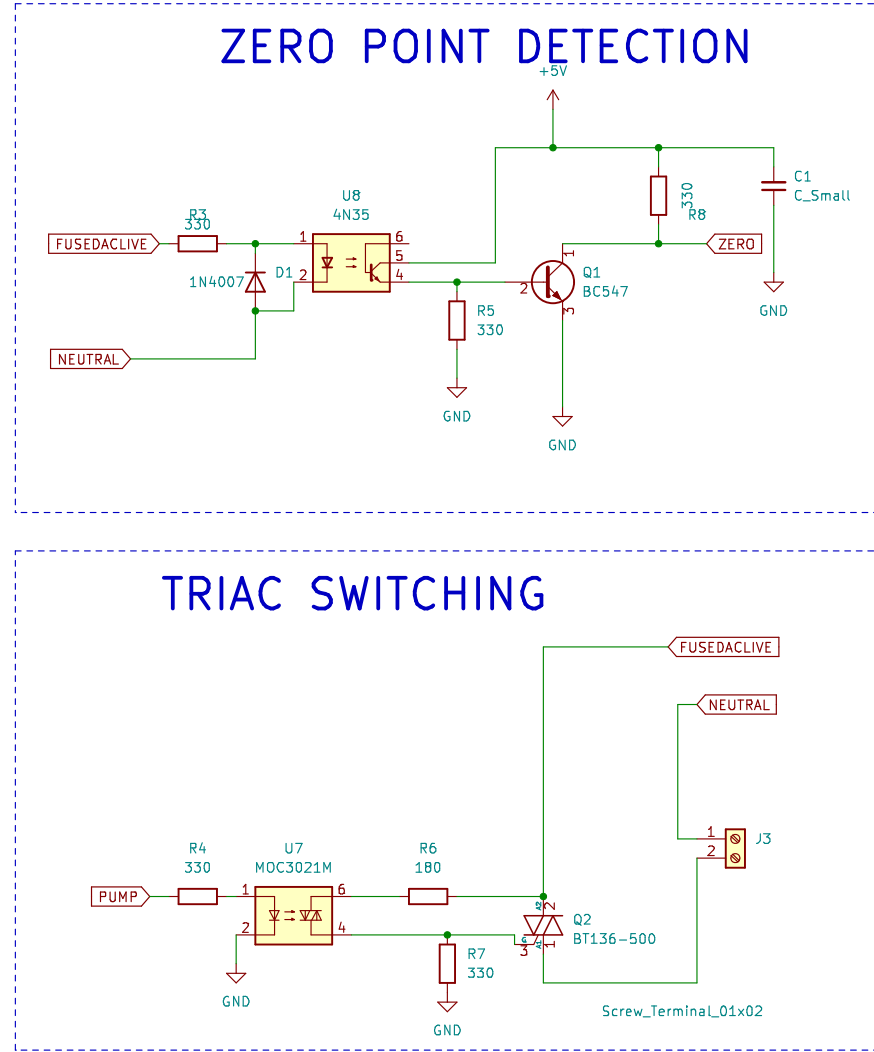


Figure 3.26: Pump circuitry

nections and the microcontroller while the second one included the pump actuation circuit.

3.3.5 Fabrication

The two Printed Circuit Boards were fabricated through etching. The circuits above were implemented using KiCad software on the schematic part of it. Based on the schematic,

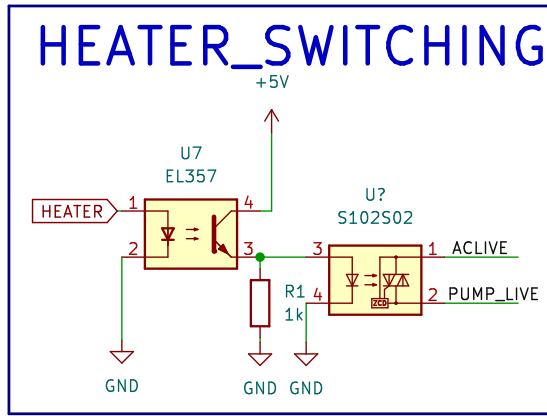


Figure 3.27: Heater circuit

these circuits were then implemented in the PCB part of KiCad and a board was generated. This board was then printed on a glossy paper in black and white using a laser jet printer. This was then transferred to a copper clad board using heat. With the rest of the copper exposed etching was carried out using cupric II chloride thereby achieving the required circuits.

3.4 Control module

The control algorithm is meant to achieve dynamic cooling of the liquid rocket engine. The control algorithm is shown in the figure below. It shows how dynamic cooling is achieved. This is done by comparing subsequent temperature values of the rocket engine's thrust chamber. In addition the change in the temperature of the coolant before and after passing through the cooling jacket is also used. Depending on the changes in the temperature the flow rate of the coolant is then varied accordingly.

4 Results and discussion

This section highlights the results from the design, fabrication and testing of the liquid engine cooling system.

4.1 Mechanical Module

4.1.1 Engine assembly

The design of the liquid rocket engine is as shown in Figure 4.1.

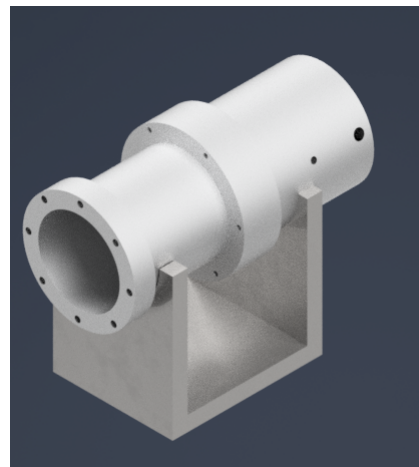


Figure 4.1: 3D Model of Liquid rocket engine

The fabricated assembly is as shown in Figure 4.2 ,Figure 4.3 and 4.4:

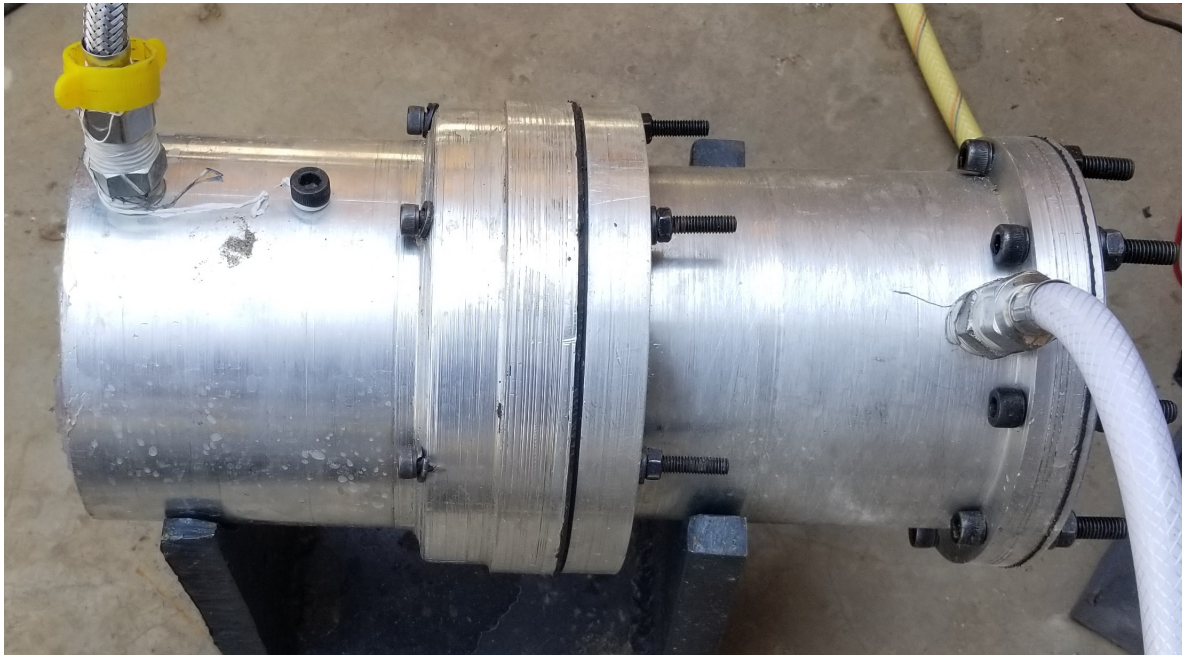


Figure 4.2: Fabricated liquid engine cooling system



Figure 4.3: Fabricated liquid engine cooling system front



Figure 4.4: Fabricated liquid engine cooling system back

4.2 Electrical Module

4.2.1 Printed Circuit Boards

The printed circuit boards were fabricated as shown in figure 4.5 and figure 4.6. The sensors PCB allowed for connection of the sensors and microcontroller. The actuation PCB has an onboard triac used for switching of the pump.

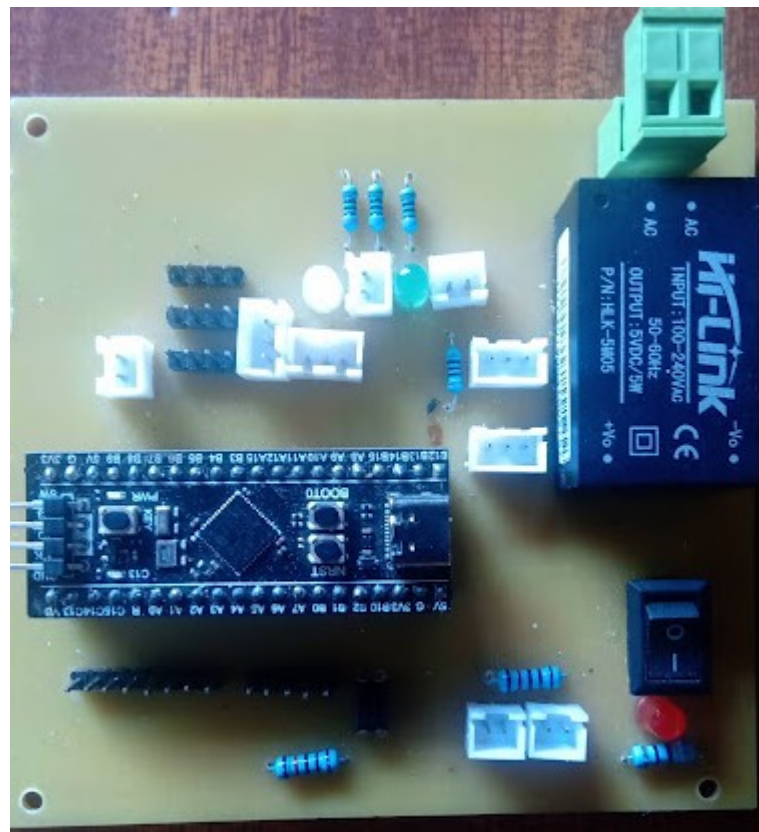


Figure 4.5: Sensors PCB



Figure 4.6: Actuation PCB

4.2.2 Casing and electronic assembly

The electronics were assembled in the casing and the results are as shown in Figure 4.7 and 4.8.

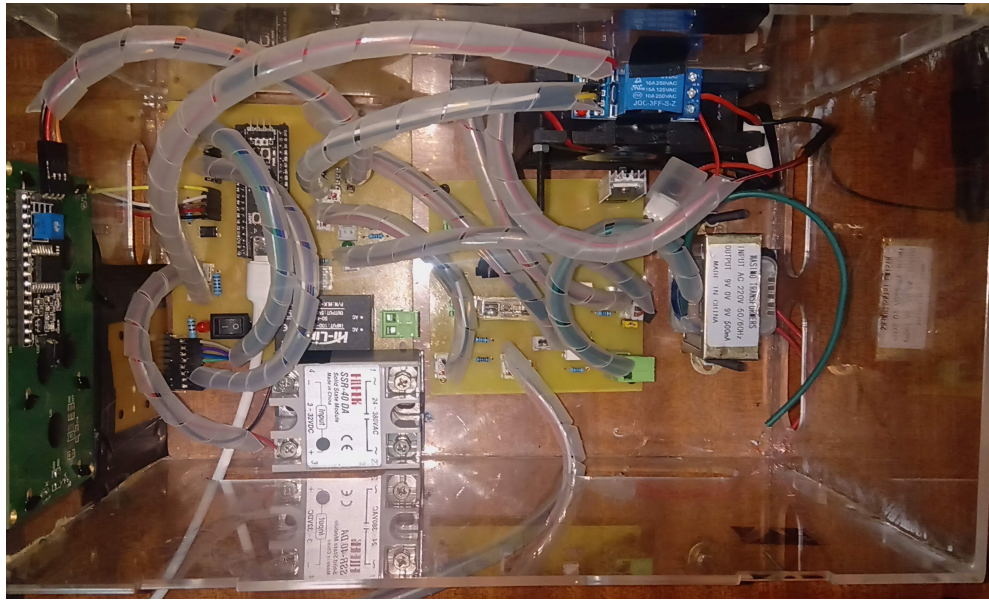


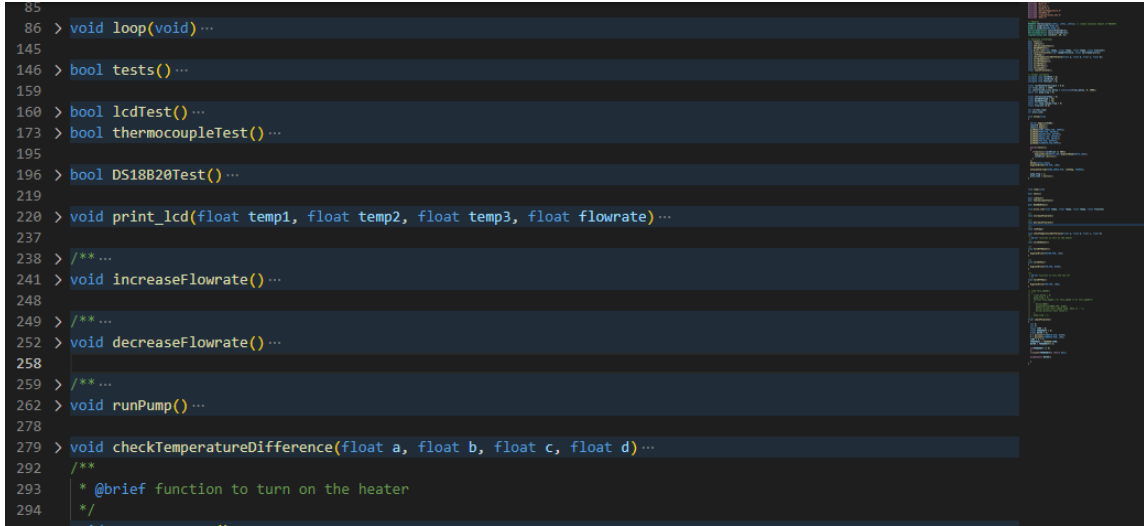
Figure 4.7: Electronics assembly-top view



Figure 4.8: Electronics assembly-front view

4.3 Control Module

The control module was implemented using the arduino framework. A snippet of the control algorithm is as shown in Figure 4.9.



```

85
86 > void loop(void) ...
145
146 > bool tests() ...
159
160 > bool lcdTest() ...
173 > bool thermocoupleTest() ...
195
196 > bool DS18B20Test() ...
219
220 > void print_lcd(float temp1, float temp2, float temp3, float flowrate) ...
237
238 > /* ...
241 > void increaseFlowrate() ...
248
249 > /* ...
252 > void decreaseFlowrate() ...
258
259 > /* ...
262 > void runPump() ...
278
279 > void checkTemperatureDifference(float a, float b, float c, float d) ...
292
293 * @brief function to turn on the heater
294 */

```

Figure 4.9: Snippet of control algorithm

The data obtained was visualized using a dashboard as shown in Figure 4.10

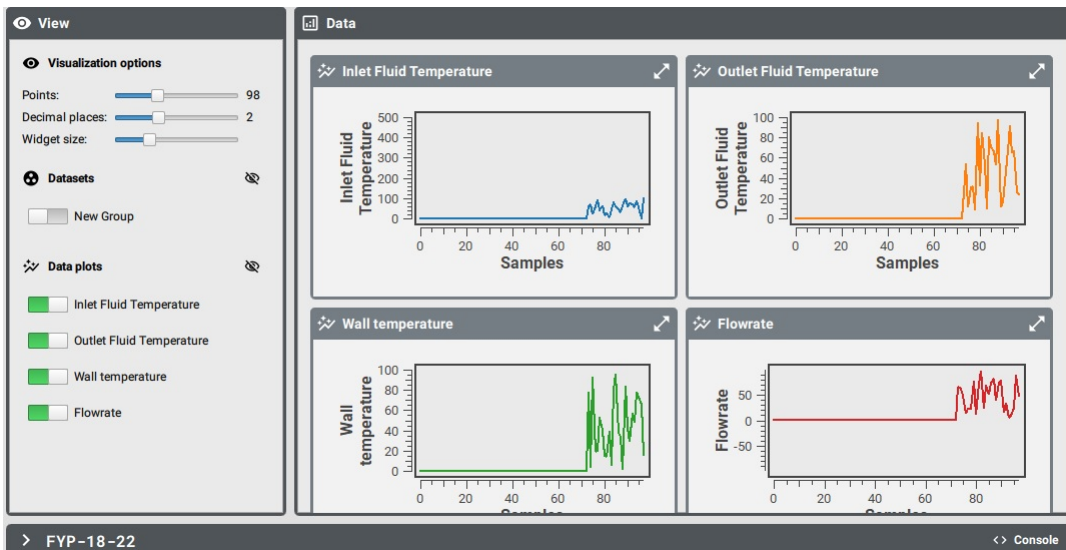


Figure 4.10: Data Visualization Dashboard

4.4 Cooling test results

A test was carried out to compare the performance of the constant flow rate cooling system versus the dynamic flow rate cooling system. The conditions of the tests as well as the results are shown in table 4.1. For both tests, the starting temperature, heating time and the time the coolant was run for were identical.

Table 4.1: Constant versus dynamic cooling results

| Cooling method | Constant cooling | Dynamic cooling |
|------------------------------------|------------------|-----------------|
| Ambient temperature(accuweather) | 24 | 25 |
| Starting temperature(thermocouple) | 26.50 | 26.50 |
| Heating with cooling time | 30 | 30 |
| Cooling time | 60 | 60 |
| Final temperature | 30.5 | 27.25 |

The ambient temperature however, was slightly more on the second run as there had to be two hours between the test to allow for the metal and the heater to return to their original temperature. However, as expected the final temperature with dynamic cooling was lower as our algorithm ensured there was an increase in coolant flow rate with rising temperatures.

4.5 Design validation

4.5.1 Fluid flow analysis

The boundary conditions used:

Table 4.2: Boundary conditions fluid flow analysis

| General setting | Density-based Analysis Energy-On |
|-----------------|-------------------------------------|
| Solver | k-e Epsilon |
| Solution type | Second order Upwind |
| Pressure | 2 Mpa |
| Temperature | 3232K |

The result are as shown:

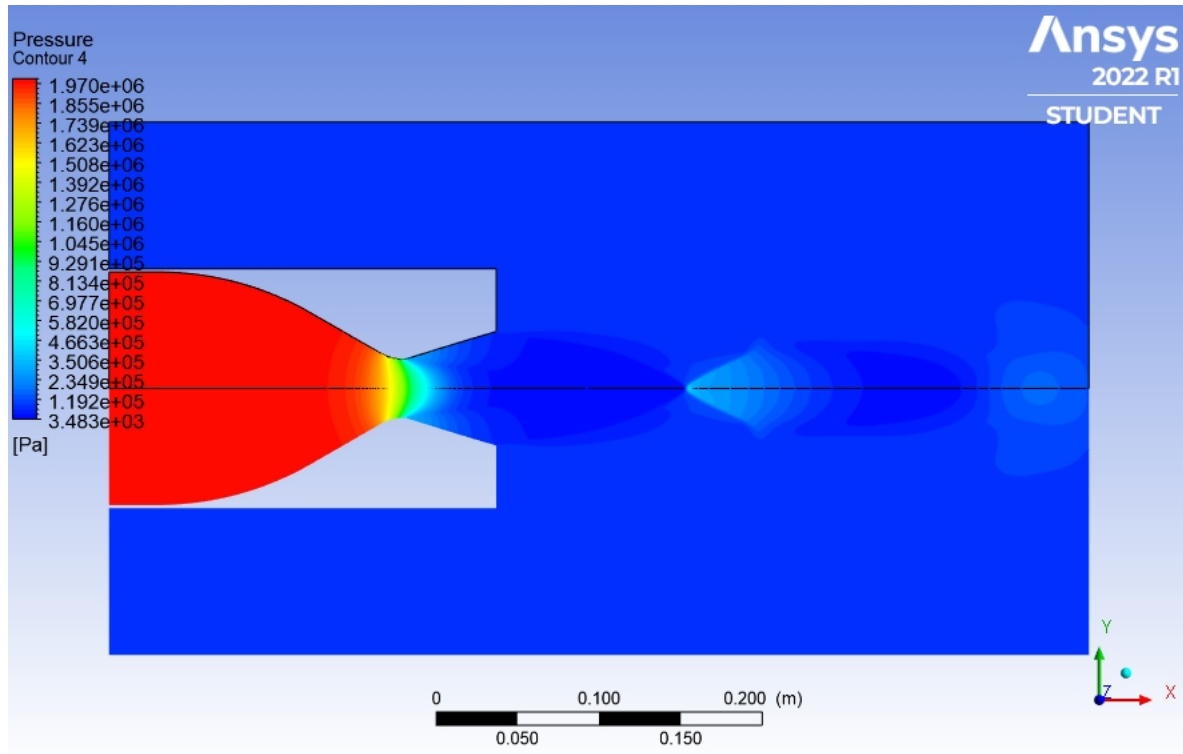


Figure 4.11: Pressure distribution

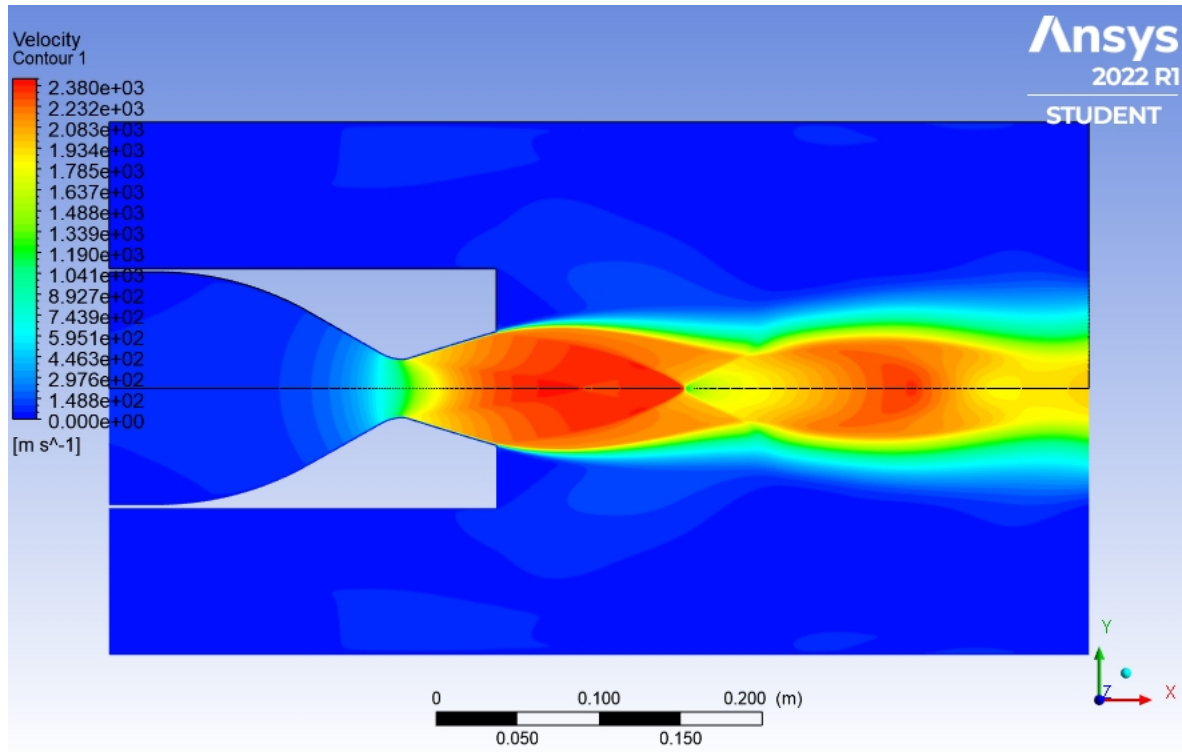


Figure 4.12: Velocity distribution

From the images above the following can be deduced:

- The exit pressure(119200Mpa) is higher than ambient pressure meaning that the flow is under-expanded. This is desired so as to eliminate issues with over-expansion such as flow separation.
- The velocity at the throat is equal to Mach 1 which is desirable.
- The velocity and pressure images do not show any shock waves.
- The exit velocity is higher than Mach 1.

Thus the designed geometry meets the required specifications.

4.5.2 Thermo-structural analysis

The boundary conditions used were as per the specifications provided by the Nakuja Project for this engine. The temperature was obtained from Nasa CEA:

Table 4.3: Boundary conditions fluid flow analysis

| | |
|-----------------|-------------------------------------|
| General setting | Density-based Analysis Energy-On |
| Solver | k-e Epsilon |
| Solution type | Second order Upwind |
| Pressure | 2 Mpa |
| Temperature | 3232K |
| Material | Stainless steel |
| Wall thickness | 2mm |

The results are shown in Figures 4.13 and 4.14

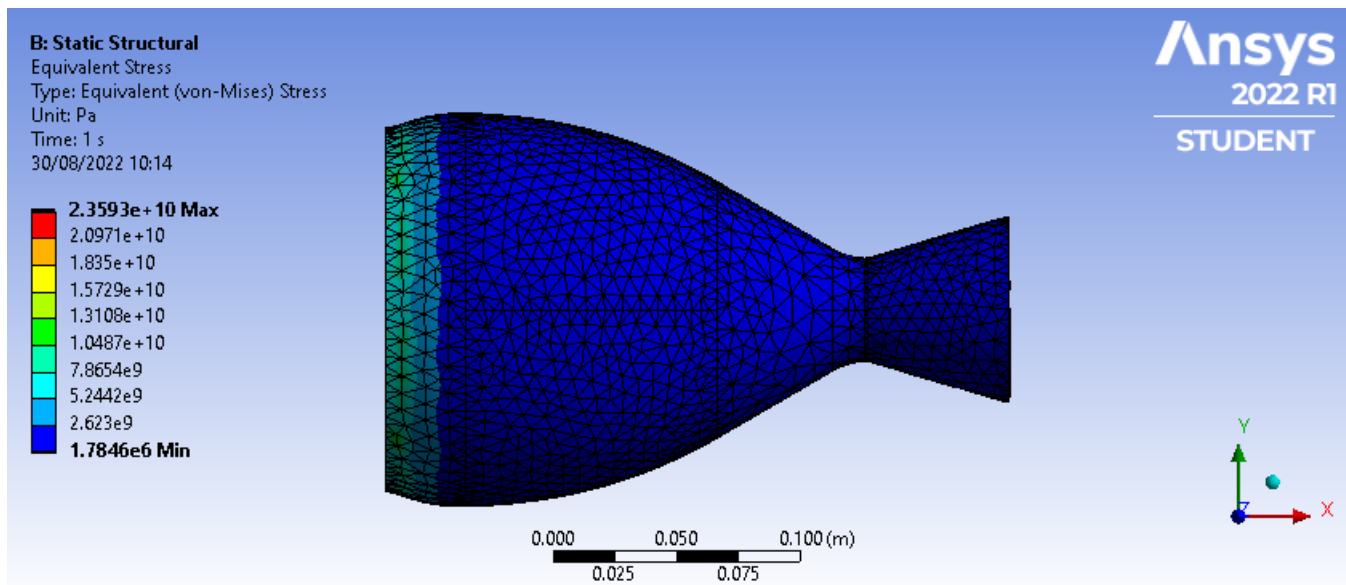


Figure 4.13: Thermo-structural analysis- Stress analysis

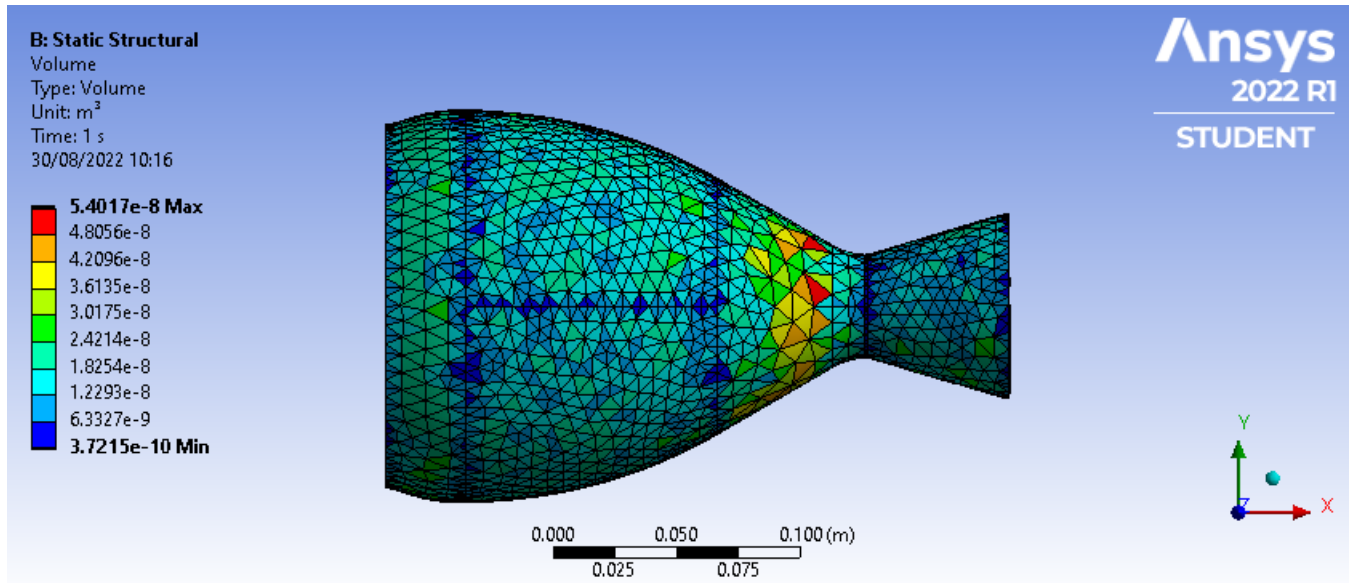


Figure 4.14: Thermo-structural analysis- Volumetric analysis

From the analysis it can be concluded that:

- The stresses experienced are below the failure point of stainless steel.
- The chosen thickness is sufficient for engine performance.

4.6 Data analysis and Discussion

The data collected showed the effectiveness of dynamic cooling over static cooling as the temperature obtained at the end was lower than that of static cooling. Dynamic cooling offers the option of better power management and stricter control of allowable temperature.

4.7 Recommendations

During the course of the tests some of the challenges encountered included:

1. Machining inaccuracies due old equipment.
2. Leakages during assembly and testing.
3. Rusting of the mild steel components
4. Delay in testing a the acquired heater took a long time to cool down.

For this the following recommendations are made:

1. Use of higher quality equipment for fabrication and maintenance of existing equipment.
2. Closer machining tolerances to avoid leakages
3. Use of stainless steel bolts for the assembly
4. Use of a ceramic heater with faster cool down.

5 Conclusion

In this project, the need to have dynamic cooling for the test bench of a liquid rocket engine was presented. A proposal was made to have dynamic cooling integrated into the cooling system of a liquid rocket engine that was also to be developed. A liquid rocket engine with regenerative cooling capacity was designed and developed.

The results of the project matched all the objectives in Section 1.3 and the expected outcomes were achieved as follows:

1. Mechanical structure with consisting of a combustion chamber, nozzle and plumbing mechanism for cooling.
2. Electrical design to power the electrical system and and transmit sensor values and control signals.
3. A control algorithm to achieve dynamic cooling.

However, the project still had a number of shortcomings from a fabrication point of view. Due to the limitations in the machining capabilities, we could not achieve the tolerances required which lead to leaks in the plumbing system. The selected method of controlling the flow rate of the pump only allowed for control of the flow rate in a limited window. The next step would be to select a better method for controlling the flow rate of the pump.

References

- [1] S. H. Youngblood, “Design and Testing of a Liquid Nitrous Oxide and Ethanol Fueled Rocket Engine,” p. 222.
- [2] M. P. Páscoa and M. Marques, “Small liquid propellant rocket engine,” 2016.
- [3] J. Hansen, “Student design of a bipropellant liquid rocket engine and associated infrastructure,” vol. 36.
- [4] D. K. Huzel and D. H. Huang, *Design of Liquid Propellant Rocket Engines*, Scientific and Technical Information Office, National Aeronautics and Space Administration [Online]. Available, 1967. [Online]. Available: <https://books.google.co.ke/books?id=UpqgnQEACAAJ>
- [5] O. B. George P. Sutton, *Rocket Propulsion Elements*, 9th ed. Wiley, 2016. [Online]. Available: libgen.li/file.php?md5=baee518e4f11a10b9506b7b66d7632c1
- [6] E. A. Santos, W. F. Alves, A. N. A. Prado, and C. A. Martins, “Development of test stand for experimental investigation of chemical and physical phenomena in liquid rocket engine,” *Journal of Aerospace Technology and Management*, vol. 3, no. 2, pp. 159–170, 2011.
- [7] T. Vinitha, S. Senthilkumar, and K. Manikandan, “Thermal Design And Analysis Of Regeneratively Cooled Thrust Chamber Of Cryogenic Rocket Engine,” *International Journal of Engineering Research*, vol. 2, no. 6, p. 8, 2013.
- [8] T. P. G. Jr, “Heating and regenerative cooling model for a rotating detonation engine designed for upper stage performance,” p. 212.
- [9] J. Poulopoulos and T. Chronopoulos, “Cooling Methods in Combustion Chambers and Nozzles,” p. 40.

- [10] S. R. Shine and S. S. Nidhi, “Review on film cooling of liquid rocket engines,” *Propulsion and Power Research*, vol. 7, no. 1, pp. 1–18, 2018.
- [11] N. A. Adams, W. Schröder, R. Radespiel, O. J. Haidn, T. Sattelmayer, C. Stemmer, and B. Weigand, Eds., *Future Space-Transport-System Components under High Thermal and Mechanical Loads: Results from the DFG Collaborative Research Center TRR40*, ser. Notes on Numerical Fluid Mechanics and Multidisciplinary Design. Cham: Springer International Publishing, 2021, vol. 146. [Online]. Available: <http://link.springer.com/10.1007/978-3-030-53847-7>
- [12] R. C. Arnold, D. Suslov, and O. J. Haidn, “Experimental investigation of film cooling with tangential slot injection in a lox/ch₄ subscale rocket combustion chamber,” *Transactions of The Japan Society for Aeronautical and Space Sciences, Space Technology Japan*, vol. 7, 2009.
- [13] G. P. Richter and T. D. Smith, “Ablative material testing for low-pressure, low-cost rocket engines,” presented at the Combustion Subcommittee, Propulsion Systems Hazards Subcommittee, Huntsville, AL, Oct, vol. 1995, Jun. 2022. [Online]. Available: <https://ntrs.nasa.gov/citations/19960007443>
- [14] M. E. Boysan, “A thesis submitted to the graduate school of natural and applied sciences of middle east technical university,” vol. 100.
- [15] J. Haemisch, D. Suslov, G. Waxenegger-Wilfing, K. Dresia, and M. Oschwald, “LUMEN – DESIGN OF THE REGENERATIVE COOLING SYSTEM FOR AN EXPANDER BLEED CYCLE ENGINE USING METHANE,” p. 10.
- [16] M. Pizzarelli, “Regenerative cooling of liquid rocket engine thrust chambers,” *Roma: Agenzia Spaziale Italiana*, 2017.
- [17] D. K. Huzel, *Modern Engineering for Design of Liquid-Propellant Rocket Engines*. AIAA, 1992.

- [18] W. Yang and B. Sun, “Numerical simulation of liquid film and regenerative cooling in a liquid rocket,” *Applied Thermal Engineering*, vol. 54, no. 2, pp. 460–469, May 2013. [Online]. Available: <https://linkinghub.elsevier.com/retrieve/pii/S1359431113001269>
- [19] A. Dhara, P. M. Kishan, and V. V. Kannah, “Design of Regenerative Cooled Cryogenic Rocket Engine,” vol. 29, no. 10, p. 19, 2020.
- [20] L. Denies, “Regenerative cooling analysis of oxygen/methane rocket engines,” p. 143.
- [21] M. Murugesan and R. Balasubramanian, “The Effect of Mass Flow Rate on the Enhanced Heat Transfer Characteristics in A Corrugated Plate Type Heat Exchanger,” *Research Journal of Engineering Sciences*, vol. 1, no. 6, pp. 22–26, 2012. [Online]. Available: <http://www.isca.in/IJES/Archive/v1/i6/4.ISCA-RJEngS-2012-097.php>
- [22] “PROPELLANTS.” [Online]. Available: <https://history.nasa.gov/conghand/propelnt.htm>
- [23] B. Smith, “Materials for rocket construction - i,” *Astronautics*, vol. 5, no. 31, pp. 7–8, June 1935.
- [24] S. Shine and S. S. Nidhi, “Review on film cooling of liquid rocket engines,” *Propulsion and Power Research*, vol. 7, no. 1, pp. 1–18, 2018.
- [25] E. Andersson, “Preliminary design of a small-scale liquid-propellant rocket engine testing platform,” 2019.
- [26] A. Elsayed, R. K. AL-Dadah, S. Mahmoud, and W. Kaialy, “Investigation of Activated Carbon / Ethanol for Low Temperature Adsorption Cooling,” p. 40.

Appendices

A Part drawings

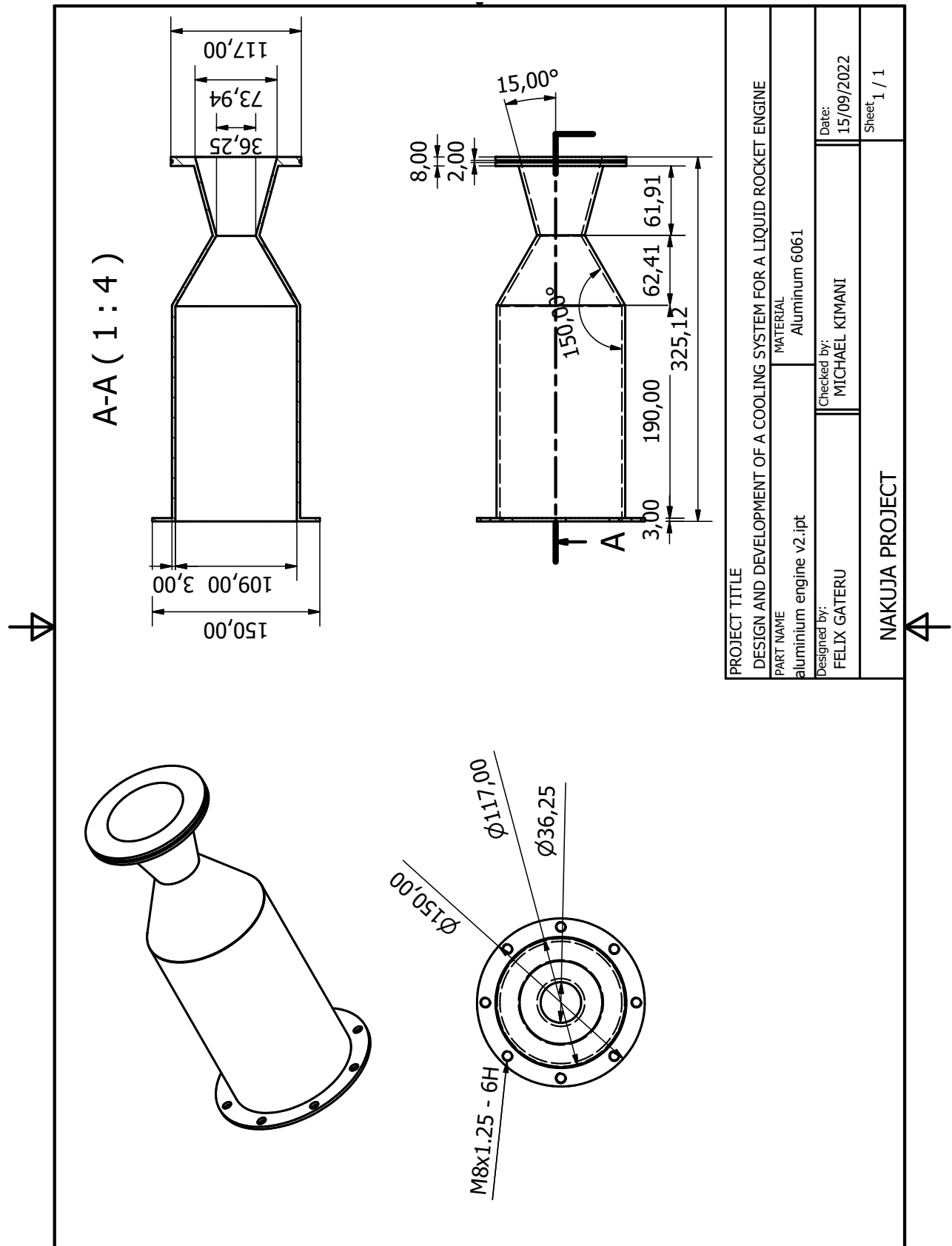


Figure A.1: Aluminium engine

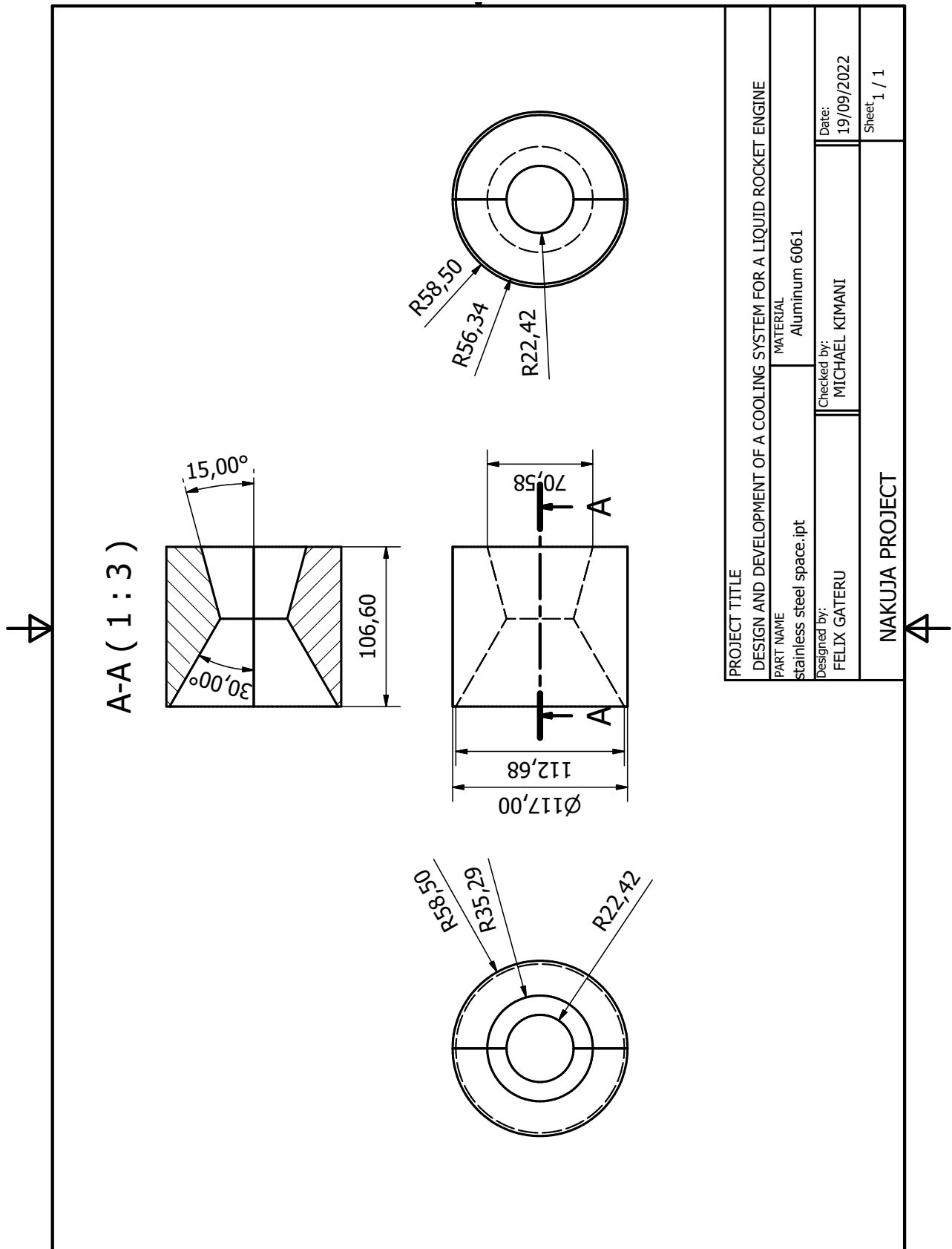


Figure A.2: Spacer

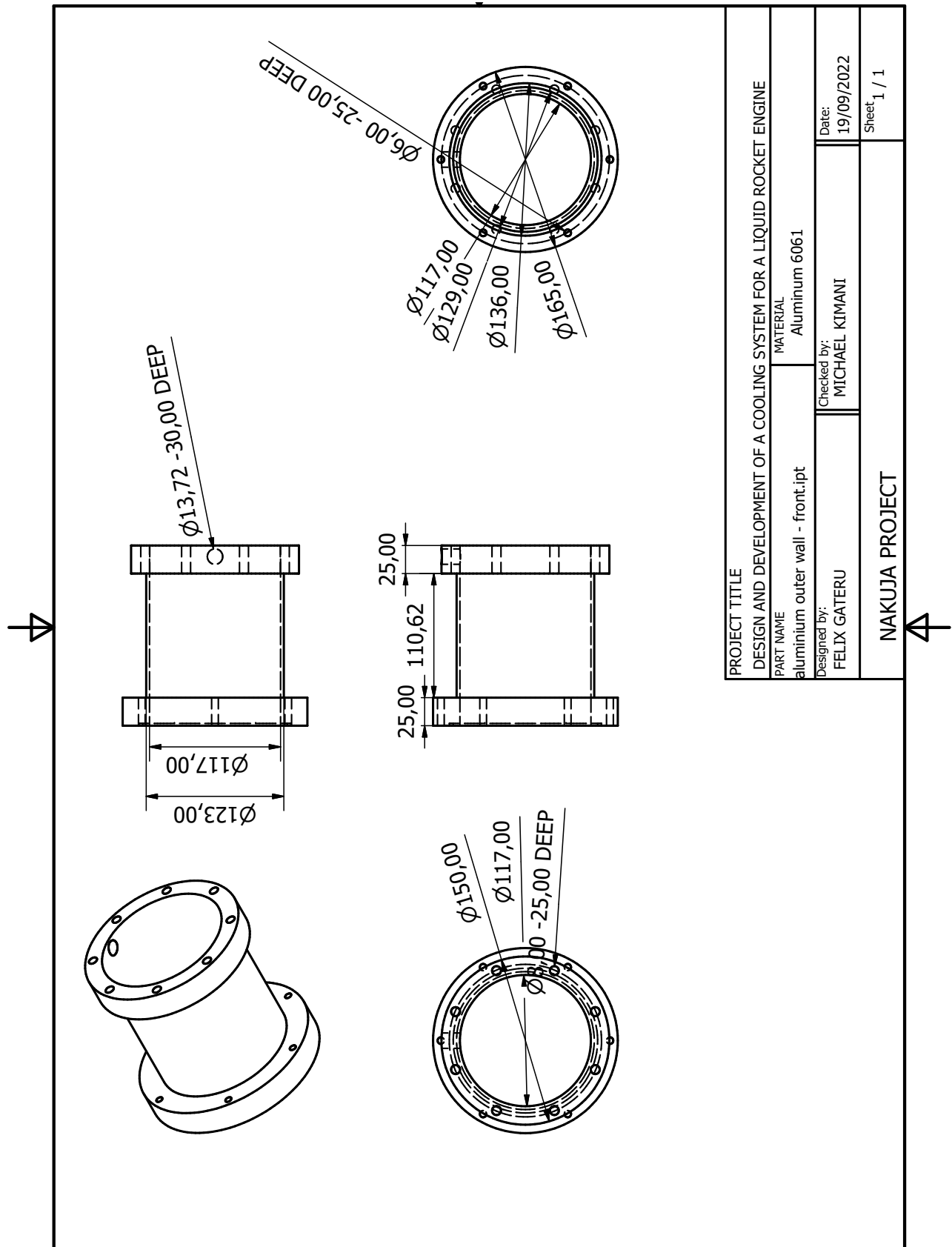


Figure A.3: Outer Wall front

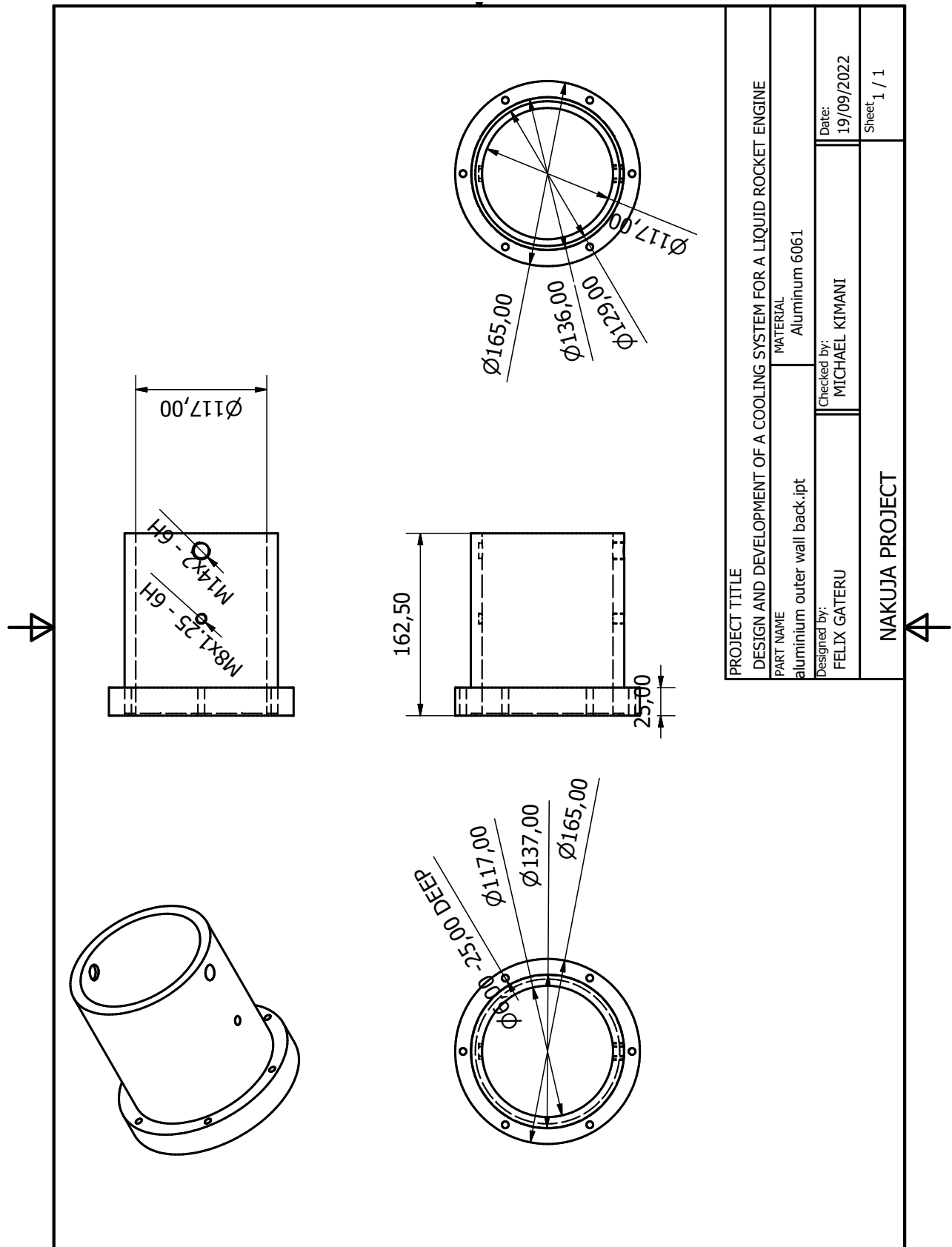


Figure A.4: Outer Wall back

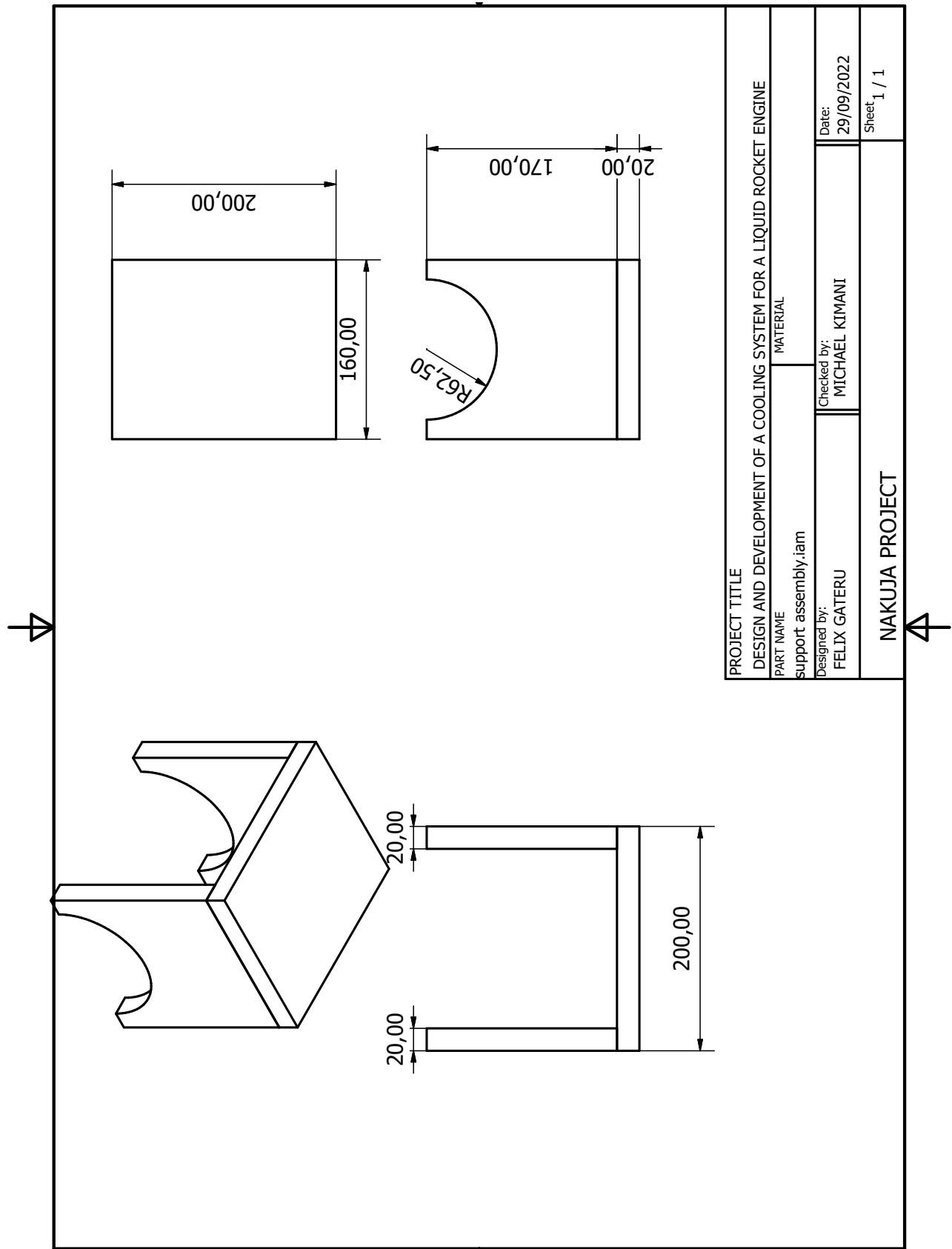


Figure A.5: Engine Support

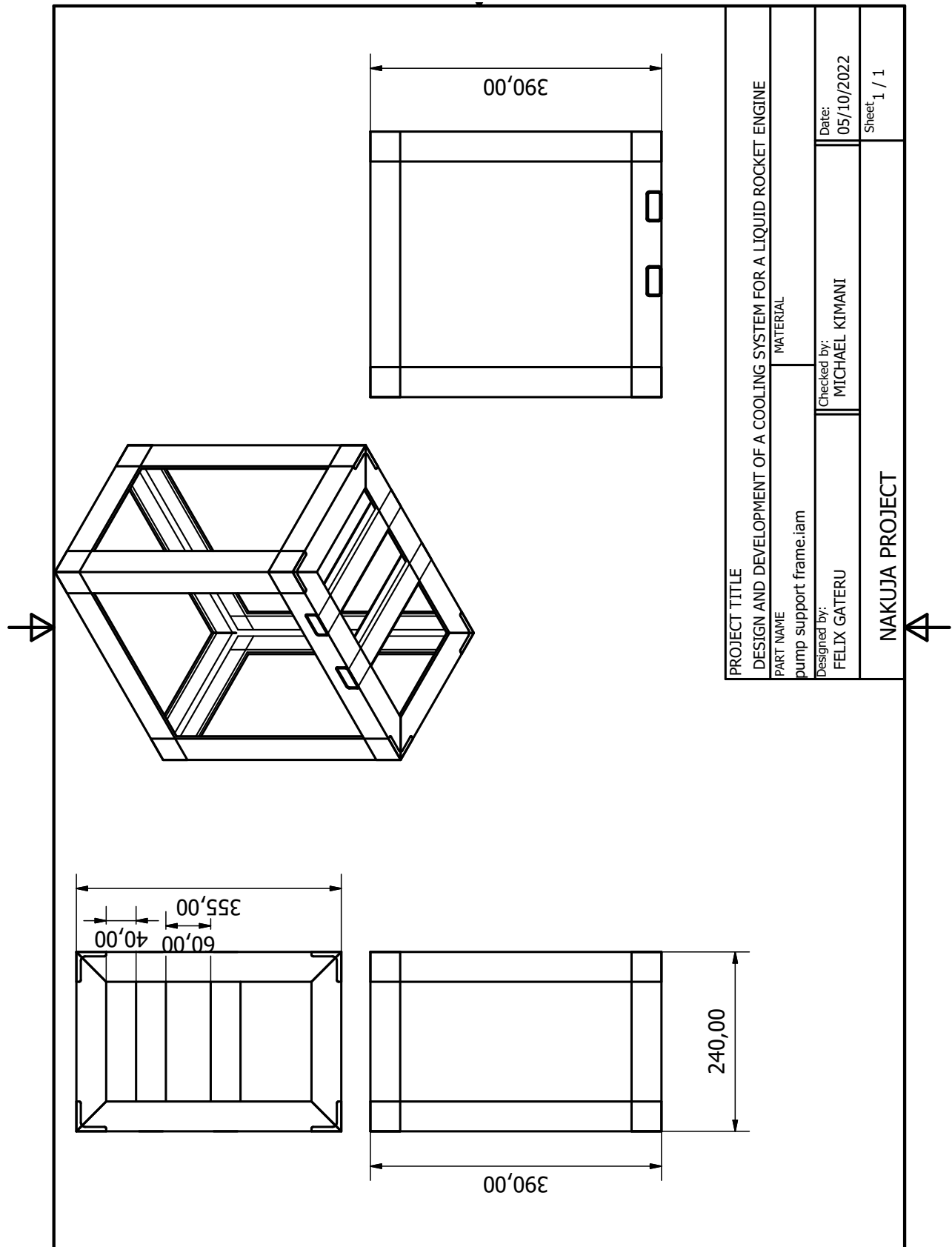


Figure A.6: Pump Support

B Bugdet and timeplan

B.1 Provisional budget

| Item | Cost per unit (KShs) | Number of components | Total Cost |
|---|----------------------|----------------------|--------------|
| Pump | 13500 | 1 | 13500 |
| Plumbing fittings | 2000 | 1 | 2000 |
| Microcontroller(ESP32) | 1400 | 1 | 1400 |
| Assorted electronics | 3000 | 1 | 3000 |
| Pressure sensors | 3000 | 2 | 6000 |
| Stainless Steel(180mm diameter billet 18metres) | 930 | 1 | 930 |
| Temperature sensors | 300 | 4 | 1200 |
| Thermocouple | 750 | 2 | 1500 |
| Flow meter | 1400 | 1 | 1400 |
| Temperature sensors | 300 | 4 | 1200 |
| Tanks | 735 | 1 | 735 |
| Mild steel(250*20*230) | 880 | 3 | 2640 |
| Total | | | 35505 |

Table B.1: Budget

B.2 Timeplan

| Week | 1 | 2 | 3 | 4 | 5 | 6 | 7 | 8 | 9 | 10 | 11 | 12 | 13 | 14 | 15 | 16 | 17 | 18 | 19 | 20 | 21 | 22 | 23 | 24 | 25 | 26 | |
|---|------|------|------|------|------|------|------|------|------|------|------|-----|-----|-----|-----|------|------|------|------|------|------|------|------|------|------|------|--|
| Proposal Presentation | Blue | Blue | | | | | | | | | | | | | | | | | | | | | | | | | |
| Literature Review | Red | Red | Red | Red | Red | Red | Red | Red | Red | Red | Red | Red | Red | Red | Red | | |
| Mechanical design | | | Blue | Blue | Blue | Blue | Blue | Blue | | | | | | | | | | | | | | | | | | | |
| Electrical and control design | | | | | | | | | Red | Red | Red | | | | | | | | | | | | | | | | |
| Continous Presentation | | | Blue | | | | | | | | | | | | | | | | |
| Interim report | | | | | | | Red | Red | Red | Red | Red | | | | | | | | | | | | | | | | |
| Mechanical fabrication | | | | | | | | | | | | | | | | Blue | Blue | Blue | Blue | Blue | Blue | | | | | | |
| Fabrication of electrical components and ssembly | | | | | | | | | | | | | | | | | Red | Red | Red | Red | Red | Red | | | | | |
| Control algorith implementation | | | | | | | | | | | | | | | | | | | | | Blue | Blue | Blue | Blue | | | |
| Assembly and testing | | | | | | | | | | | | | | | | | | Red | Red | Red | Red | | | | | | |
| Final Presentation | | | | | | | | | | | | | | | | | | | | | | | | Blue | Blue | Blue | |

Table B.2: Time plan

C Programming Code

C.1 CEA output parser-Python code

```

import matplotlib.pyplot as plt
import pandas as pd
import numpy as np
import os
import sys

def annot_max(x,y, ax=None):
    xmax = x[np.argmax(y)]
    ymax = y.max()
    text= "x={:.3f}, y={:.3f}".format(xmax, ymax)
    if not ax:
        ax = plt.gca()
    loc = ax.get_loc('top')
    ax.plot([xmax], [ymax], 'ro')
    ax.text(xmax, ymax, text, va='bottom', ha='left', loc=loc)
    return ax

```

```
ax=plt.gca()

bbox_props = dict(boxstyle="square",pad=0.3, fc="w", ec="k", lw=0.72)
arrowprops=dict(arrowstyle="->",connectionstyle="angle,angleA=0,angleB=60")
kw = dict(xycoords='data',textcoords="axes fraction",
          arrowprops=arrowprops, bbox=bbox_props, ha="right", va="top")
ax.annotate(text, xy=(xmax, ymax), xytext=(0.94,0.96), **kw)

file_name = input("Please input the file name:\n")
fuel_name = input("Please input the name of the fuel:\n")
file = open(os.path.join(sys.path[0],file_name)).read()
outputs = file.split('THEORETICAL')
outputs = outputs[1:]
df = pd.DataFrame()
Of_ratio = []
Imp = []
Kelvin = []
Mass_flux_ratio = []
for output in outputs:
    dic = {}
    Pin = output.split('Pin =')[1].split('PSIA')[0].strip()
    O_F = output.split('O/F=')[1].split('%FUEL')[0].strip()
    Temp = output.split('T, K')[1].split('RHO')[0].strip().split()[0]
    flux = output.split('M, (1/n)')[1].split('(dLV/dLP)t')[0].strip().split()[0]
    Isp = output.split('Isp, M/SEC')[1].split('MOLE')[0].strip().split()[1]
    #dic['Pin'] = float(Pin)
    #dic['O_F'] = float(O_F)
    #dic['Isp'] = float(Isp)/9.
```

```
Of_ratio.append(float(0_F))
Imp.append(float(Isp)/9.81)
Kelvin.append(float(Temp))
Mass_flux_ratio.append(float(Temp)/float(flux))

#dic['Temp'] = float(Temp)

df1 = pd.DataFrame(dic, index=[0])
df = pd.concat([df, df1], ignore_index=True)

#Pins = list(df['Pin'].unique())
#colors = ['o-r', 'o-b', 'o-g', 'o-c', 'o-m', 'o-y', 'o-k', 'o-r', 'o-
b', 'o-g', 'o-c', 'o-m', 'o-y', 'o-k']
#cnt = 0

#for Pin in Pins:
#    color = colors[cnt]
#    val = df[df['Pin']==Pin]
#    plt.plot(val['0_F'],val['Isp'],color)
#    plt.plot(val['0_F'],val['Temp'],color)
#    cnt += 1

#plt.legend([str(Pin)+(psia) for Pin in Pins])
#plt.xlabel('0/F ratio')
#plt.ylabel('Isp')
#plt.show()

fig, axs = plt.subplots(2)
```

```
fig.suptitle(f'{fuel_name} plus gas oxygen')

axs[0].plot(Of_ratio,Kelvin)
axs[0].set(ylabel='Temp(K)')
axs[0].set_title('Temperature against oxodizer-fuel ratio')

axs[1].plot(Of_ratio,Isp)
axs[1].set(ylabel='Isp(s)')
axs[1].set_title('Temperature against oxodizer-fuel ratio')

annot_max(np.array(Of_ratio),np.array(Kelvin))

#plt.plot(Of_ratio,Mass_flux_ratio) to plot ratio of heat to molar mass

plt.show()
```

C.2 Nozzle sizing code-Matlab code

```
%Chemistry

% Ethanol GOX


%Ddesign Point
Mftot = 0.71254 %kg/s
Ofratio = 1.5
Pc = 2*10^6 %Pa
Pe = 101800 %Pa
%Characteristic length
Lc = 1.43%m


%From NASA CEA
Tc = 3232.42 %K
```

```
%propellants molar mass
```

```
M = 22.035 %kg/kmol
```

```
Gamma = 1.2032
```

```
%From universal gas constant
```

```
R = 414.66
```

```
%Ry
```

```
Ry = 8314*Gamma
```

```
%Throat area
```

```
At = (Mftot/Pc)*sqrt(Tc*R/Gamma)*(1+(Gamma -1)/2)^((Gamma+1)/(2*(Gamma -1)))
```

```
%Throat diameter
```

```
Dt = 2 * sqrt(At/3.142)
```

```
%Exit Mach Number
```

```
Me = sqrt((2*((Pe/Pc)^-(((Gamma -1)/Gamma))-1))/(Gamma-1))
```

```
%Let Ar be the ratio Ae/At
```

```
Ar = (1/Me)*((2/(Gamma+1))*(1+(((Gamma-1)/2))*Me^2))^((Gamma+1)/(2*(Gamma-1)))
```

```
%Area of exit
```

```
Ae = At * Ar
```

```
%Exit area diameter
```

```
De = 2 * sqrt(Ae/3.142)
```

```
%Exit velocity
```

```
Ue = sqrt(2 * Ry/(Gamma-1)*(Tc/M) * (1 - (Pe/Pc)^((Gamma-1)/Gamma)))
```

```
%Specific Impulse
```

```
Isp = Ue/9.8
```

```
%Thrust
```

```
F = Mftot * Ue
```

```
%Chamber volume
```

```
Vc = At * Lc
```

```
Ac = At * (8*((Dt*100)^-0.6) + 1.25)
```

```
%Actual chamber length
```

```
Lch = Vc / Ac
```

```
Dc = 2 * sqrt(Ac/3.142)
```

```
%Ending point
```

```
%Lc = 0.17
```

```
%Dc = 0.054
```

```
%Nozzle expanding at 15 degrees
```

```
theta_n = 15
```

```
Ln = (De-Dt)/(2*tand(theta_n))
```

C.3 Main control logic- C++ Code

```
#include <Arduino.h>
#include <Wire.h>
#include <string.h>
#include "OneWire.h"
#include "DallasTemperature.h"
#include "max6675.h"
#include "LiquidCrystal_I2C.h"
#include "defs.h"

// Objects
MAX6675 thermocouple(sckPin, csPin, soPin); // create instance object of MAX6675
OneWire oneWire(ONE_WIRE_0);
OneWire oneWire1(ONE_WIRE_1);
DallasTemperature sensor0(&oneWire);
DallasTemperature sensor1(&oneWire1);
LiquidCrystal_I2C lcd(0x27, 20, 4);

// function prototypes
bool tests();
bool lcdTest();
bool thermocoupleTest();
bool DS18B20Test();
void print_lcd(float temp1, float temp2, float temp3);
void controlFlowrate(float tempDifference, float wallTemperature);
```

```
//Global variables
unsigned long lastRead = 0;
float thermocoupleTemp = 0.0;
float DS18B20Temp0 = 0.0;
float DS18B20Temp1 = 0.0;
int pumpSpeed = 0;

void setup(void)
{
    Serial.begin(115200);
    sensor0.begin();
    sensor1.begin();
    tests();
    pinMode(PUMP_PIN,OUTPUT);
    pinMode(HEATER_PIN,OUTPUT);
}

void loop(void)
{
    sensor0.requestTemperatures();
    sensor1.requestTemperatures(); // Send the command to get temperature readings
                                // Serial.println("DONE");
    /*****************************************************************/
    float thermocoupleTemp = thermocouple.readCelsius();
    float DS18B20Temp0 = sensor0.getTempCByIndex(0);
    float DS18B20Temp1 = sensor1.getTempCByIndex(0);

    Serial.print("C = ");
```

```
Serial.println(thermocoupleTemp);
Serial.print("Temp 1 is: ");
Serial.println(DS18B20Temp0);
Serial.print("Temp 2 is: ");
Serial.println(DS18B20Temp1);
runPump();
checkTemperatureDifference(DS18B20Temp0,DS18B20Temp1);
if(millis()-lastRead >= 1000){
    print_lcd(thermocoupleTemp,DS18B20Temp0,DS18B20Temp1);
    lastRead=millis();
}
}

bool tests()
{
    while (!lcdTest())
    {
    }
    while (!thermocoupleTest())
    {
    }
    while (!DS18B20Test())
    {
    }
    return true;
}
```

```
bool lcdTest()
{
    lcd.init();
    lcd.backlight();
    lcd.print("Maya v0.0.1");
    lcd.setCursor(7,3);
    lcd.print("FYP 18-22");
    delay(1000);
    lcd.clear();
    lcd.print("Starting tests ..... ");
    delay(1000);
    return true;
}

bool thermocoupleTest()
{
    lcd.clear();
    lcd.print("Running thermocouple test!!!!");
    int count = 0;
    while (count < 10)
    {
        delay(100);
        if (thermocouple.readCelsius() > 0 && thermocouple.readCelsius() < 50)
        {
            count++;
        }
        else
        {
            continue;
        }
    }
}
```

```
    }

}

lcd.clear();

lcd.println("Thermocouple test complete !!!!!!!");

delay(1000);

return true;

}

bool DS18B20Test()

{

lcd.clear();

lcd.println("Running DS18B20 test !!!!!!!");

delay(1000);

int count = 0;

while (count < 10)

{

    delay(100);

    if (sensor0.getTempCByIndex(0) > 0 && sensor0.getTempCByIndex(0) < 50 && sensor1.g

    {

        count++;

    }

    else

    {

        continue;

    }

}

lcd.clear();

lcd.println("DS18B20 test complete.....!!!!!!");

delay(1000);
```

```
    return true;
}

void print_lcd(float temp1, float temp2, float temp3){
    lcd.clear();
    lcd.setCursor(0,0);
    lcd.print("Thermocouple: ");
    lcd.print(temp1);
    lcd.setCursor(0,1);
    lcd.print("Probe 1: ");
    lcd.print(temp2);
    lcd.setCursor(0,2);
    lcd.print("Probe 2: ");
    lcd.print(temp3);

}

/***
 * @brief function to log data
 */
void logData(){

}

/***
 * @brief function to increase flowrate according to temperature
 */
void increaseFlowrate(){
    //implement increased flowrate
}
```

```
}

/** 
 * @brief function to decrease flowrate.
 */
void decreaseFlowrate(){

}

/** 
 * @brief function to run the pump.
 */
void runPump(){
    // TO IMPLEMENT RUN PUMP

}

void checkTemperatureDifference(float a, float b){
    if(a-b>10){
        increaseFlowrate();
    }
    else if (a-b<0){
        decreaseFlowrate();
    }

}

/** 
 * @brief function to turn on the heater

```

```
*/  
void turnOnHeater(){  
    digitalWrite(HEATER_PIN,HIGH);  
  
}  
  
/**  
 * @brief function to turn off the heater  
 */  
void turnOffHeater(){  
    digitalWrite(HEATER_PIN,LOW);  
  
}  
  
/**  
 * @brief Function to turn on the fan  
 */  
void turnOnFan(){  
    digitalWrite(FAN_PIN,HIGH);  
}  
  
/**  
 * @brief Function to turn the fan off  
 * */  
void turnOffFan(){  
    digitalWrite(FAN_PIN,LOW);  
}
```

D Design reference tables, charts